Dalton Transactions

Antiproliferative activity of a series of cisplatin-based Pt(IV)-acetylamido/carboxylato prodrugs

Journal:	*Dalton Transactions*
Manuscript ID	DT-ART-12-2015-004905.R1
Article Type:	Paper
Date Submitted by the Author:	n/a
Complete List of Authors:	Ravera, Mauro; University of Piemonte Orientale, DiSIT Gabano, Elisabetta; University of Piemonte Orientale, DiSIT Zanellato, Ilaria; University of Piemonte Orientale, DiSIT Fregonese, Federico; University of Piemonte Orientale, DiSIT Pelosi, Giorgio; Universita degli studi di Parma, Dipartimento di Chimica Platts, James; Cardiff University, School of Chemistry Osella, Domenico; University of Piemonte Orientale, DiSIT

Dalton Transactions

Guidelines to Referees

Communications & Papers

The international journal for inorganic, organometallic and bioinorganic chemistry

http://www.rsc.org/dalton

Dalton Transactions wishes to encourage high quality articles reporting exciting new developments in inorganic chemistry.

For an article to be accepted, it must report new, high-quality research and make a significant contribution to the field.

Manuscripts which describe purely physical, crystallographic or computational studies must include the clear relevance of the work to the broad inorganic chemistry readership of *Dalton Transactions*.

Communications must report chemistry of sufficient importance and impact to justify preliminary publication. **Papers** should report more complete studies.

***Dalton Transactions* Impact Factor is 4.19** (2014 Journal Citation Reports®)

Routine or unnecessarily fragmented work, however competently researched and reported, should not be recommended for publication.

Thank you very much for your assistance in evaluating this manuscript

Dr Andrew Shore (dalton@rsc.org)
Royal Society of Chemistry
Editor, *Dalton Transactions*

Professor Philip Mountford
University of Oxford
Chair, *Dalton Transactions* Editorial Board

General Guidance (for further details, see the RSC Refereeing Procedure and Policy)

When preparing your report, please:

- Comment on the **originality**, **importance**, **impact** and **scientific reliability** of the work
- State clearly whether you would like to see the paper accepted or rejected and give detailed comments (with references, as appropriate) that will help both the Editor to make a decision on the paper and the authors to improve it

Please inform the Editor if:

- There is a conflict of interest
- There is a significant part of the work which you are not able to referee with confidence
- If the work, or a significant part of the work, has previously been published, including online publication (*e.g.* on a preprint server/open access server)
- You believe the work, or a significant part of the work, is currently submitted elsewhere
- The work represents part of an unduly fragmented investigation

UNIVERSITÀ DEL PIEMONTE ORIENTALE

PROF. DOMENICO OSELLA, *FRSC*

DIPARTIMENTO DI SCIENZE E INNOVAZIONE TECNOLOGICA

Viale Teresa Michel 11 – 15121 Alessandria
Tel. 0131 360266 – Fax 0131 360250
domenico.osella@uniupo.it

D. Osella et al. " *Antiproliferative activity of a series of cisplatin-based Pt(IV)-acetylamido/carboxylato prodrugs*"

DT-ART-12-2015-004905

Response to Referees

Referee: 1

The introduction part needs to be further expanded to facilitate the reading especially for the readers outside the field. For example, the current status of biologically active asymmetric Pt(IV) prodrugs needs to be mentioned, i.e., why it is important to develop new asymmetric Pt(IV) prodrugs that are biologically active.

In the Introduction the importance of developing new asymmetric Pt(IV) prodrugs has been explained in the context of drug targeting and delivery.

The water solubility of complexes 2a-5a and 2b-5b should be measured and the numbers should be included in SI.

The water solubility have been measured and the data have been included in the ESI.

For the stability tests by NMR, the original NMR spectra should be included in SI and proper comparisons should be made.

The original NMR spectra have been added in the SI.

For the reduction tests by HPLC in the presence of ascorbic acid, the original HPLC chromatograms of other compounds should also be included to support the conclusions on P6, right column, 2nd paragraph.

The HPLC chromatograms for the reductions of all the compounds have been added in the ESI.

It is very interesting to see that the acetylamido complex undergoes reduction to have cisplatin as the major product and cis-[Pt(acetylamido-N)Cl(NH_3)$_2$] as the by-product. What's the implication of this process on the biological activity of the acetylamido complexes compared with that of carboxylato prodrugs? Will the replacement of Cl with acetylamido group decrease the cytotoxicity since the by-product is a monofunctional Pt(II) compound?

The implication of this side process is now amply discussed in the text along with the appropriate references.

The original E_p values should be tabulated in the manuscript.

The E_p values have been added in the ESI.

The real numbers for the IC_{50} values should be included in Fig. 3.

The IC_{50} values have been moved from SI to Fig. 3.

"Accumulation ratio" should be clearly defined in the maintext.

The accumulation ratio is now clearly defined in the text.

The advantages of having acetylamido Pt(IV) prodrugs rather than carboxylato ones should be emphasized in the conclusion, e.g., their good solubility and stability under light.

The advantages of the new series of compounds have more emphasized in the conclusions.

Referee: 2

on page 5, line 68, is written: "the X-ray structure of 3b, reported in ...Figure 1". According to Scheme 1 the compound should be 3a and not 3b.

The label **3b** has been replaced in all cases in which it refers to the crystal structure with **3a** in the main text and in the supplementary information.

Figure 1, reported in the same page, clearly shows a H-bond (dashed line) between O1 and N1. This is visually wrong and contrasts with what is stated on line 89 of the same page (5): "intramolecular hydrogen bond with N2".

The Referee is totally right: the drawing has been corrected.

The authors suggest that the oxidation takes place via a radical mechanism which can well be, but in this case I would expect an effect of light which is not taken into account.

Unfortunately, we have not investigated in deep the effect of the light in the original reaction: all the syntheses, including that of **1a** were carried out in vessels wrapped with aluminum foils.

It appears that the Pt(IV) complexes are intrinsically less cytotoxic than the Pt(II) counterparts and only for the most lipophilic derivatives the increased uptake of the Pt(IV) species can compensate for their intrinsic smaller activity. In the abstract is stated that the derivatives with longer chains are more active against A2780 ovarian cancer cells than cisplatin. This does not appear to be the case from inspection of Figure 3 (particularly if one takes into account the intrinsic uncertainty of this type of measurements).

The Referee is totally right: we put too emphasis in the original sentence in the abstract that has been reformulated as: "For those with longer chains and hence greater cell uptake, this difference is negated and acetylamido complexes are as active as acetato analogues, both exhibiting antiproliferative potency ($1/IC_{50}$) against A2780 ovarian cancer cells similar to that of cisplatin."

Moreover, in Figure 3 are reported in the ordinate negative values of IC50, which is just a non sense.

It has been corrected.

Minor points:
Page 2, line 57: delete the second "peaks".
Page 3, line 79: delete [M+H]+.
Page 5, lines 77-78: An angle cannot be close to linearity. The sentence can be rearranged in the following way: "The arrangement of the axial ligands is very close to linearity (N3-Pt1-O2 angle of 175.6(2)°).
Page 7, line 84: "2-5 pairs" could be better than "2-5 couples".

All this typos have been corrected.

Crystallographic Referee: 3

There is 1 Structure in this paper. We examined this file: CCDC-1442209.

It is mentioned in the text that "All the non-hydrogen atoms in the molecules were refined anisotropically." This is not so - C(5) and C(6) were isotropic. I tried anisotropic refinement on them (see 3b.res attached). it yields enormous thermal ellipsoids, but consistent with dynamic disorder of this group. I recommend to follow this refinement, and the resulting Checkcif alerts to be ignored.

Also, the orientations of methyl and amino-groups can be optimised (AFIX 137).

We have tried the anisotropic refinement, but given the checkcif warning that could alarm non-crystallographers, we decided to stick to the isotropic version.

Following the recommendations of Referee 3, we have rerun a final anisotropic refinement in which we also allowed the rotation of the methyls and of the amino groups using the AFIX 137 option. All the data in the text and the supplementary materials have accordingly been updated.

We wish to thank the Referee for his careful checking and his useful suggestions.

Cite this: DOI: 10.1039/c0xx00000x

www.rsc.org/xxxxxx

PAPER

Antiproliferative activity of a series of cisplatin-based Pt(IV)-acetylamido/carboxylato prodrugs

Mauro Ravera,[a] Elisabetta Gabano,[a] Ilaria Zanellato,[a] Federico Fregonese,[a] Giorgio Pelosi,[b] James A. Platts,[c] and Domenico Osella,*[a]

Received (in XXX, XXX) Xth XXXXXXXXX 20XX, Accepted Xth XXXXXXXXX 20XX
DOI: 10.1039/b000000x

We report studies of a novel series of Pt(IV) complexes exhibiting an asymmetric combination of acetylamido and carboxylato ligands in the axial positions. We demonstrate efficient synthesis of a series of analogues, differing in alkyl chain length and hence lipophilicity, from a stable acetylamido/hydroxido complex formed by reaction of cisplatin with peroxyacetimidic acid (PAIA). NMR spectroscopy and X-ray crystallography confirm the identity of the resulting complexes, and highlight subtle differences in structure and stability of acetylamido complexes compared to equivalent acetato complexes. Reduction of acetylamido complexes, whether achieved chemically or electro-chemically, is significantly more difficult than of acetate complexes, resulting in lower antiproliferative activity for shorter-chain complexes. For those with longer chains and hence greater cell uptake, this difference is negated and acetylamido complexes are as active as acetato analogues, both exhibiting antiproliferative potency ($1/IC_{50}$) against A2780 ovarian cancer cells similar to that of cisplatin.

Introduction

Platinum(IV) complexes have been raised in the last decade as a possible alternative to the traditional platinum(II)-based anticancer drugs because of their potential advantages over the latter. Platinum(IV) complexes are quite inert toward ligand substitution and therefore avoid off-target reactions that deactivate Pt(II) complexes and contribute to their side effects. Pt(IV) compounds can reach the tumour site intact, where they are activated through reaction with endogenous reductants, like ascorbate, glutathione or proteins (activation by reduction).[1] Bioreduction of Pt(IV) complexes leads to the corresponding cytotoxic square-planar Pt(II) species by releasing usually both axial ligands. The equatorial ligands determine the nature and activity of the final metabolite, whereas the two axial ligands provide additional opportunities for the tuning of the lipophilicity and the rate of reduction of such Pt(IV) prodrugs.[2, 3] Additionally, the axial ligands can play an important role in the drug targeting and delivery (DTD) strategy.[3-6] Pt(IV) derivatives bearing succinic acid/s in axial position/s are well suited for this purpose, since one carboxylic group is axially linked to the Pt core while the second is available for further reactions with the designed biovector (active DTD) or with the designed nanoparticle (passive DTD), through amide or ester bond. Using dihydroxido Pt(IV) synthons for the esterification reaction with the designed with succinic anhydride, disuccinato Pt(IV) complexes are easily obtained. They can react with one or two designed biovectors often giving mixtures of molecules difficult to be separated, or large aggregates of uncontrolled dimensions in the case of reaction with nanoparticles.[7] Thus, monofunctional (asymmetric) Pt(IV) derivatives are highly desired for such a purpose.[8]

In an attempt to obtain mono-hydroxido Pt(IV) synthons with a chemically inert second axial ligand, the Radziszewski reaction has been recently applied to the synthesis of a new class of Pt(IV) complexes.[9] This method is based on the reaction between acetonitrile and hydrogen peroxide that forms the reactive intermediate peroxyacetimidic acid, PAIA (Scheme 1). PAIA provides a hydroxido and an acetylamido ligand, the latter being *N*-coordinated during the Pt(II)→Pt(IV) oxidation step. The resulting (*OC*-6-44)-(acetylamido-*N*)diamminedichloridohydroxidoplatinum(IV), **1a**, is highly soluble and very stable in water and represents an interesting building block for the further development of Pt(IV) antitumor prodrug candidates. For this purpose, the reactivity of complex **1a** towards different anhydrides and/or activated carboxylic acids has been studied leading to the synthesis of compounds **2a**-**5a** (Scheme 1). The newly synthesized complexes were tested *in vitro* on A2780 ovarian cancer cells. Finally, a series of monoacetato Pt(IV) analogues was added to compare the chemical and biological results (series **b**, Scheme 2).

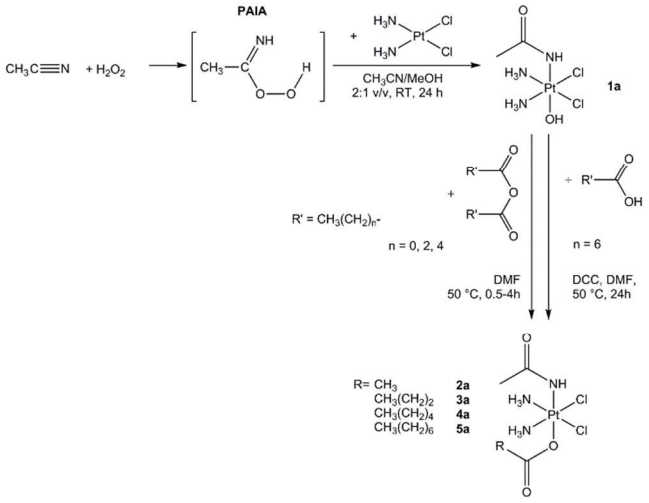

Scheme 1. Reaction scheme for the synthesis of the acetylamido complexes **1a**-**5a** (DCC = dicyclohexycarbodiimide)

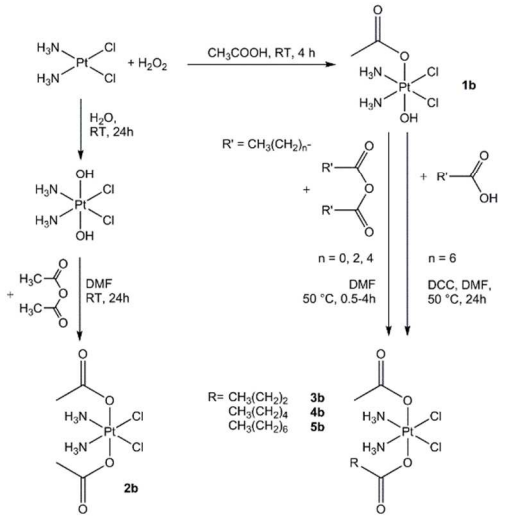

Scheme 2. Reaction scheme for the synthesis of the acetato complexes **1b**-**5b** (DCC = dicyclohexycarbodiimide)

Experimental section

Materials and methods

$K_2[PtCl_4]$ (Johnson Matthey and Co.) and all other chemicals (Aldrich) were used without further purification. (*SP*-4-2)-diamminedichloridoplatinum(II) (*i.e.*, cisplatin, *cis*-$[PtCl_2(NH_3)_2]$),[10] (*OC*-6-33)-diacetatodiamminedichloridoplatinum(IV), **2b**[11], and (*SP*-4-3)-(acetylamido-*N*)diamminechloridoplatinum(II) (*i.e.*, *cis*-[Pt(acetylamido-*N*)Cl$(NH_3)_2$])[12] were synthesized according to literature procedures. The synthesis of **1a** has been recently reported by us,[9] whereas **1b** was synthesized by slight modifications of a previously reported procedure.[13] Complexes **1a** and **1b** were also synthesized using $^{15}NH_3$ to be used in mechanistic studies. All reactions were carried out in aluminum-foil-wrapped vessels.

The purity of the compounds was assessed by analytical RP-HPLC, elemental analysis and determination of Pt content by inductively coupled plasma-optical emission spectrometry (ICP-OES). Elemental analyses were carried out with an EA3000 CHN Elemental Analyzer (EuroVector, Milano, Italy). Platinum was quantified by means of a Spectro Genesis ICP-OES spectrometer (Spectro Analytical Instruments, Kleve, Germany) equipped with a crossflow nebulizer. In order to quantify the platinum concentration the Pt 299.797 nm line was selected. A platinum standard stock solution of 1000 mg L^{-1} was diluted in 1.0% v/v nitric acid to prepare calibration standards.

NMR spectra were measured on a Bruker Advance III NMR spectrometer operating at 500 (^{1}H), 125.7 (^{13}C), 107.2 (^{195}Pt), and 50.7 MHz (^{15}N), respectively. ^{1}H and ^{13}C NMR chemical shifts were reported in parts per million (ppm) referenced to solvent resonances. ^{195}Pt NMR spectra were recorded using a solution of $K_2[PtCl_4]$ in saturated aqueous KCl as the external reference. The shift for $K_2[PtCl_4]$ was adjusted to -1628 ppm from $Na_2[PtCl_6]$ (δ = 0 ppm). ^{15}N NMR spectra were recorded using a solution of $^{15}NH_4Cl$ in 1 M HCl as the external reference. [^{1}H, ^{15}N] HSQC spectra (Heteronuclear Single Quantum Correlation) were obtained with the standard Bruker sequence hsqcetgpsiz with 0.2 s acquisition time, 8 scans, 1.3 s relaxation delay, and 128 F_1 points. DEPT-45 (Distortionless Enhancement by Polarization Transfer) spectra were recorded with 100 scans, 3.5 s relaxation delay, 0.5 s acquisition time and 75 Hz for ^1J (^{15}N, ^{1}H).

RP-HPLC and mass analysis were performed using a Waters HPLC-MS instrument equipped with Alliance 2695 separations module, 2487 dual lambda absorbance detector. The chromatographic conditions were: silica-based C18 stationary phase (5-µm Phenomenex Phenosphere-NEXT C18 column 250×4.6 mm ID), mobile phase containing 15 mM HCOOH aqueous solution and CH_3OH in different ratios depending on the complex, flow rate = 0.5 mL min^{-1} (isocratic elution), UV-visible detector set at 210 nm. Electrospray ionization mass spectra (ESI-MS) were obtained setting the source and desolvation temperatures to 150 °C and 250 °C, respectively, and using nitrogen both as a drying and a nebulizing gas. The cone and the capillary voltages were usually 30 V or 20 V and 2.70 kV, respectively. Quasi-molecular ion peaks $[M+H]^+$ were assigned on the basis of the *m/z* values and of the simulated isotope distribution patterns.

An Autolab PGSTAT12 electrochemical analyser (Eco Chemie, Utrecht, The Netherlands) interfaced to a personal computer running GPES 4.9 electrochemical software was used for the electrochemical measurements. A standard three-electrode cell was designed to allow the tip of the reference electrode (Ag/AgCl, 3M KCl) to closely approach the working electrode (a glassy carbon, GC, disk, diameter 0.1 cm, sealed in epoxy resin). The GC working electrode was polished with alumina, then rinsed with distilled water and dried. This process yielded an almost completely reproducible surface for all experiments. All measurements were carried out under nitrogen in ethanol solutions containing 0.1 M $[NBu_4][ClO_4]$ as supporting electrolyte and the metal complexes 0.50 mM. All potentials are reported *vs.* Ag/AgCl, 3 M KCl. Positive-feedback iR compensation was applied routinely.

Synthesis of complexes 2a-4a. Complex **1a** (100 mg, 0.266 mmol) was suspended in DMF (10 mL) at 50 °C and after 5 min a 10-fold excess of anhydride (2.66 mmol, *i.e.* 272 mg of acetic anhydride, 422 mg of butyric anhydride, or 570 mg of hexanoic anhydride) was added. The reaction mixture was stirred at 50 °C

until suspension became clear (0.5-4 h). The resulting solution was filtered, the solvent removed under reduced pressure and the residue triturated with diethyl ether.

2a. Yield: 111 mg (93%). Elemental analysis: found C, 11.2; H, 3.4; N, 10.3; Pt, 46.5%. Calc. for $C_4H_{13}Cl_2N_3O_3Pt$ C, 11.5; H, 3.1; N, 10.1; Pt, 46.8%. ^{1}H NMR (500 MHz, d_6-DMSO) δ: 1.88 (s, 3H, Pt-O-CO-CH_3), 1.93 (s, 3H, Pt-NH-CO-CH_3), 5.28 (s, 1H, Pt-NH-CO-CH_3), 6.48 (m, 6H, NH_3) ppm. ^{13}C NMR (125.7 MHz, d_6-DMSO) δ: 23.9 (Pt-O-CO-*C*H_3), 24.9 (Pt-NH-CO-*C*H_3), 175.5 (Pt-NH-*C*O-CH_3), 178.3 (Pt-O-*C*O-CH_3) ppm. ^{195}Pt NMR (107.2 MHz, d_6-DMSO) δ: 496 ppm. ESI-MS (positive ion mode): found 418.3 *m/z*. Calc. for $[C_4H_{14}Cl_2N_3O_3Pt]^+$ 418.0 *m/z* $[M+H]^+$.

3a. Yield: 108 mg (91%). Elemental analysis: found C, 16.0; H, 4.0; N, 9.7; Pt, 44.0%. Calc. for $C_6H_{17}Cl_2N_3O_3Pt$ C, 16.2; H, 3.85; N, 9.4; Pt, 43.8%. ^{1}H NMR (500 MHz, d_6-DMSO) δ: 0.88 (t, J = 7.4 Hz, 3H, Pt-O-CO-CH_2-CH_2-CH_3), 1.49 (q, J = 7.4 Hz, 2H, Pt-O-CO-CH_2-CH_2-CH_3), 1.92 (s, 3H, Pt-NH-CO-CH_3), 2.14 (t, J = 7.4 Hz, 2H, Pt-O-CO-CH_2-CH_2-CH_3), 5.16 (s, 1H, Pt-NH-CO-CH_3), 6.48 (m, 6H, NH_3) ppm. ^{13}C NMR (125.7 MHz, d_6-DMSO) δ: 13.8 (Pt-O-CO-CH_2-CH_2-*C*H_3), 18.9 (Pt-O-CO-CH_2-*C*H_2-CH_3), 25.1 (Pt-NH-CO-*C*H_3), 38.6 (Pt-O-CO-*C*H_2-CH_2-CH_3), 175.5 (Pt-NH-*C*O-CH_3), 180.8 (Pt-O-*C*O-CH_2-CH_2-CH_3) ppm. ^{195}Pt NMR (107.2 MHz, d_6-DMSO) δ: 496 ppm. ESI-MS (positive ion mode): found 446.3 *m/z*. Calc. for $[C_6H_{18}Cl_2N_3O_3Pt]^+$ 446.0 *m/z* $[M+H]^+$.

4a. Yield: 109 mg (87%). Elemental analysis: found C, 20.0; H, 4.1; N, 8.6; Pt, 41.0%. Calc. for $C_8H_{21}Cl_2N_3O_3Pt$ C, 20.3; H, 4.5; N, 8.9; Pt, 41.2%. ^{1}H NMR (500 MHz, d_6-DMSO) δ: 0.86 (t, J = 6.9 Hz, 3H, Pt-O-CO-CH_2-CH_2-CH_2-CH_2-CH_3), 1.26 (m, 4H, Pt-O-CO-CH_2-CH_2-CH_2-CH_2-CH_3), 1.47 (m, 2H, Pt-O-CO-CH_2-CH_2-CH_2-CH_2-CH_3), 1.92 (s, 2H, Pt-NH-CO-CH_3), 2.15 (t, J = 7.4 Hz, 2H, Pt-O-CO-CH_2-CH_2-CH_2-CH_2-CH_3), 5.16 (s, 1H, Pt-NH-CO-CH_3), 6.52 (m, 6H, NH_3) ppm. ^{13}C NMR (125.7 MHz, d_6-DMSO) δ: 13.9 (Pt-O-CO-CH_2-CH_2-CH_2-CH_2-*C*H_3), 22.0 (Pt-O-CO-CH_2-CH_2-CH_2-*C*H_2-CH_3), 25.1 (Pt-NH-CO-*C*H_3), 25.2 (Pt-O-CO-CH_2-*C*H_2-CH_2-CH_2-CH_3), 31.0 (Pt-O-CO-CH_2-CH_2-*C*H_2-CH_2-CH_3), 36.6 (Pt-O-CO-*C*H_2-CH_2-CH_2-CH_2-CH_3), 175.5 (Pt-NH-*C*O-CH_3), 180.9 (Pt-O-*C*O-CH_2-CH_2-CH_2-CH_2-CH_3) ppm. ^{195}Pt NMR (107.2 MHz, d_6-DMSO) δ: 496 ppm. ESI-MS (positive ion mode): found 474.1 *m/z*. Calc. for $[C_8H_{22}Cl_2N_3O_3Pt]^+$ 474.1 *m/z* $[M+H]^+$.

Synthesis of complex 5a. A solution of n-octanoic acid (258 mg, 1.8 mmol) and dicyclohexylcarbodiimide (DCC, 371 mg, 1.8 mmol) in DMF (2 mL) was put in ultrasonic bath for 15 min at room temperature. After sonication, the filtered solution was added dropwise to a suspension of **1a** (112 mg, 0.3 mmol) in 2 ml of DMF. The reaction mixture was stirred for 24 h at 50 °C. Solvent was partially removed under reduced pressure and 20 mL of diethyl ether were added to obtain **5a** as a pale yellow powder. Yield: 87 mg (65%). Elemental analysis: found C, 24.4; H, 4.7; N, 8.1; Pt, 39.3%. Calc. for $C_{10}H_{25}Cl_2N_3O_3Pt$ C, 24.0; H, 5.0; N, 8.4; Pt, 39.0%. ^{1}H NMR (500 MHz, d_6-DMSO) δ: 0.86 (t, J = 6.5 Hz, 3H, Pt-O-CO-CH_2-CH_2-CH_2-CH_2-CH_2-CH_2-CH_3), 1.25 (m, 8H, Pt-O-CO-CH_2-CH_2-CH_2-CH_2-CH_2-CH_2-CH_3), 1.46 (m, 2H, Pt-O-CO-CH_2-CH_2-CH_2-CH_2-CH_2-CH_2-CH_3), 1.92 (s, 2H, Pt-NH-CO-CH_3), 2.15 (t, J = 7.5 Hz, 2H, Pt-O-CO-CH_2-CH_2-CH_2-CH_2-CH_2-CH_2-CH_3), 5.16 (s, 1H, Pt-NH-CO-CH_3), 6.47 (m, 6H, NH_3) ppm. ^{13}C NMR (125.7 MHz, d_6-DMSO) δ: 13.9 (Pt-O-CO-CH_2-CH_2-CH_2-CH_2-CH_2-CH_2-*C*H_3), 22.1 (Pt-O-CO-CH_2-CH_2-*C*H_2-CH_2-CH_2-CH_2-CH_3), 25.1 (Pt-NH-CO-*C*H_3), 25.5 (Pt-O-CO-CH_2-CH_2-CH_2-CH_2-CH_2-*C*H_2-CH_3), 28.6-28.7 (Pt-O-CO-CH_2-CH_2-CH_2-*C*H_2-CH_2-CH_2-CH_3), 31.2 (Pt-O-CO-CH_2-*C*H_2-CH_2-CH_2-*C*H_2-CH_2-CH_3), 36.6 (Pt-O-CO-*C*H_2-CH_2-CH_2-CH_2-*C*H_2-CH_2-CH_3), 175.5 (Pt-NH-*C*O-CH_3), 180.9 (Pt-O-*C*O-CH_2-CH_2-CH_2-CH_2-CH_2-CH_3) ppm. ^{195}Pt NMR (107.2 MHz, d_6-DMSO) δ: 496 ppm. ESI-MS (positive ion mode): found 502.2 *m/z*. Calc. for $[C_{10}H_{26}Cl_2N_3O_3Pt]^+$ 502.1 *m/z* $[M+H]^+$.

Synthesis of complex 1b. Cisplatin (100 mg, 0.33 mmol) was suspended in acetic acid (40 mL) and H_2O_2 50% w/w (1 mL, 35 mmol) was added. The reaction mixture was stirred at room temperature until the solution becomes clear (ca. 3 h). The solution was filtered, the solvent removed under reduced pressure, and the residue triturated with diethyl ether to obtain **1b** as a pale yellow solid. Yield: 110 mg (88%). Elemental analysis: found C, 6.6; H, 3.0; N, 7.2; Pt, 51.6%. Calc. for $C_2H_{10}Cl_2N_2O_3Pt$ C, 6.4; H, 2.7; N, 7.45; Pt, 51.9%. ^{1}H NMR (500 MHz, d_6-DMSO) δ: 1.91 (s, 3H, CH_3), 5.93 (t with ^{195}Pt satellites peaks, $^1J_{H\text{-}N}$ = 52.9 Hz, $^2J_{H\text{-}Pt}$ = 53.0 Hz, 6H, NH_3) ppm. ^{13}C NMR (125.7 MHz, d_6-DMSO) δ: 23.7 (CH_3), 178.4 (Pt-O-CO) ppm. ^{195}Pt NMR (107.2 MHz, d_6-DMSO) δ: 1041 ppm. ESI-MS (positive ion mode): found 377.3 (47%) and 359.0 (100%) *m/z*. Calc. for $[C_2H_{11}Cl_2N_2O_3Pt]^+$ 377.0 $[M+H]^+$ and $[C_2H_9Cl_2N_2O_2Pt]^+$ 359.0 $[M\text{-}OH]^+$ *m/z*.

Synthesis of complexes 3b and 4b. Complex **1b** (100 mg, 0.266 mmol) was suspended in DMF (10 mL) at 50 °C and after 5 min a 10-fold excess of anhydride (2.66 mmol, *i.e.* 422 mg of butyric anhydride, or 570 mg of hexanoic anhydride or 266 mg of succinic anhydride) was added. The reaction mixture was stirred at 50 °C until suspension becomes clear (0.5-4 h). The resulting solution was filtered, the solvent removed under reduced pressure and the residue triturated with diethyl ether.

3b. Yield: 106 mg (90%). Elemental analysis: found C, 16.4; H, 3.5; N, 6.5; Pt, 43.4%. Calc. for $C_6H_{16}Cl_2N_2O_4Pt$ C, 16.15; H, 3.6; N, 6.3; Pt, 43.7%. ^{1}H NMR (500 MHz, d_6-DMSO) δ: 0.87 (t, 3H, J = 7.4 Hz, Pt-O-CO-CH_2-CH_2-CH_3), 1.47 (q, 2H, J = 7.4 Hz, Pt-O-CO-CH_2-CH_2-CH_3), 1.90 (s, 3H, Pt-O-CO-CH_3), 2.19 (t, 2H, J = 7.4 Hz, Pt-O-CO-CH_2-CH_2-CH_3), 6.52 (m, 6H, NH_3) ppm. ^{13}C NMR (125.7 MHz, d_6-DMSO) δ: 13.6 (Pt-O-CO-CH_2-CH_2-*C*H_3), 18.8 (Pt-O-CO-CH_2-*C*H_2-CH_3), 22.9 (Pt-O-CO-*C*H_3), 37.7 (Pt-O-CO-*C*H_2-CH_2-CH_3), 178.2 (Pt-O-*C*O-CH_3), 180.8 (Pt-O-*C*O-CH_2-CH_2-CH_3) ppm. ^{195}Pt NMR (107.2 MHz, d_6-DMSO) δ: 1224 ppm. ESI-MS (positive ion mode): found 447.3 *m/z*. Calc. for $[C_6H_{17}Cl_2N_2O_4Pt]^+$ 447.0 *m/z* $[M+H]^+$.

4b. Yield: 107 mg (85%). Elemental analysis: found C, 20.0; H, 4.5; N, 5.9; Pt, 41.3%. Calc. for $C_8H_{20}Cl_2N_2O_4Pt$ C, 20.3; H, 4.25; N, 5.9; Pt, 41.1%. ^{1}H NMR (500 MHz, d_6-DMSO) δ: 0.86 (t, J = 7.0 Hz, 3H, Pt-O-CO-CH_2-CH_2-CH_2-CH_2-CH_3), 1.26 (m, 4H, Pt-O-CO-CH_2-CH_2-CH_2-CH_2-CH_3), 1.45 (m, 2H, Pt-O-CO-CH_2-CH_2-CH_2-CH_2-CH_3), 1.90 (s, 2H, Pt-O-CO-CH_3), 2.20 (t, J = 7.4 Hz, 2H, Pt-O-CO-CH_2-CH_2-CH_2-CH_2-CH_3), 6.52 (m, 6H, NH_3) ppm. ^{13}C NMR (125.7 MHz, d_6-DMSO) δ: 13.9 (Pt-O-CO-CH_2-CH_2-CH_2-CH_2-*C*H_3), 21.9 (Pt-O-CO-CH_2-CH_2-CH_2-*C*H_2-CH_3), 22.9 (Pt-O-CO-*C*H_3), 25.1 (Pt-O-CO-CH_2-*C*H_2-CH_2-CH_2-CH_3), 30.8 (Pt-O-CO-CH_2-CH_2-*C*H_2-CH_2-CH_3), 35.6 (Pt-O-CO-*C*H_2-CH_2-CH_2-CH_2-CH_3), 178.2 (Pt-O-*C*O-CH_3), 180.9 (Pt-O-*C*O-CH_2-CH_2-CH_2-CH_2-CH_3) ppm. ^{195}Pt NMR (107.2 MHz, d_6-

DMSO) δ: 1223 ppm. ESI-MS (positive ion mode): found 475.1 *m/z*. Calc. for $[C_8H_{21}Cl_2N_2O_4Pt]^+$ 475.0 *m/z* $[M+H]^+$.

Synthesis of complex 5b. A solution of n-octanoic acid (258 mg, 1.8 mmol) and DCC (371 mg, 1.8 mmol) in DMF (2 mL) was put in ultrasonic bath for 15 min at room temperature. After sonication, the filtered solution was added dropwise to a suspension of **1b** (113 mg, 0.3 mmol) in 2 ml of DMF. The reaction mixture was stirred for 24 h at 50 °C. Solvent was partially removed under reduced pressure and 20 mL of diethyl ether were added to obtain **5b** as a pale yellow powder. Yield: 82 mg (61%). Elemental analysis: found C, 24.1; H, 5.3; N, 5.5; Pt, 38.9%. Calc. for $C_{10}H_{24}Cl_2N_2O_4Pt$ C, 23.9; H, 4.8; N, 5.6; Pt, 38.8%. ^{1}H NMR (500 MHz, d_6-DMSO) δ: 0.86 (t, J = 6.8 Hz, 3H, Pt-O-CO-CH_2-CH_2-CH_2-CH_2-CH_2-CH_2-CH_3), 1.25 (m, 8H, Pt-O-CO-CH_2-CH_2-CH_2-CH_2-CH_2-CH_2-CH_3), 1.45 (m, 2H, Pt-O-CO-CH_2-CH_2-CH_2-CH_2-CH_2-CH_2-CH_3), 1.90 (s, 2H, Pt-O-CO-CH_3), 2.20 (t, J = 7.4 Hz, 2H, Pt-O-CO-CH_2-CH_2-CH_2-CH_2-CH_2-CH_2-CH_3), 6.47 (m, 6H, NH_3) ppm. ^{13}C NMR (125.7 MHz, d_6-DMSO) δ: 14.4 (Pt-O-CO-CH_2-CH_2-CH_2-CH_2-CH_2-CH_2-CH_3), 22.6 (Pt-O-CO-CH_2-CH_2-CH_2-CH_2-CH_2-CH_3), 23.4 (Pt-O-CO-CH_3), 24.9 (Pt-O-CO-CH_2-CH_2-CH_2-CH_2-CH_2-CH_2-CH_3), 25.8 (Pt-O-CO-CH_2-CH_2-CH_2-CH_2-CH_2-CH_3), 29.0 (Pt-O-CO-CH_2-CH_2-CH_2-CH_2-CH_2-CH_2-CH_3), 31.7 (Pt-O-CO-CH_2-CH_2-CH_2-CH_2-CH_2-CH_2-CH_3), 36.2 (Pt-O-CO-CH_2-CH_2-CH_2-CH_2-CH_2-CH_2-CH_3), 178.7 (Pt-O-CO-CH_3), 181.4 (Pt-O-CO-CH_2-CH_2-CH_2-CH_2-CH_2-CH_2-CH_3) ppm. ^{195}Pt NMR (107.2 MHz, d_6-DMSO) δ: 1223 ppm. ESI-MS (positive ion mode): found 503.2 *m/z*. Calc. for $[C_{10}H_{25}Cl_2N_2O_4Pt]^+$ 503.1 *m/z* $[M+H]^+$.

Synthesis of $^{15}NH_3$-containing complexes 1a and 1b. The syntheses of complexes **1a** and **1b** containing ^{15}N ammonia were the same of those containing $^{14}NH_3$,[9, 13] but starting from *cis*-$[PtCl_2(^{15}NH_3)_2]$.[14] The relevant characterization data are reported below.

(^{15}N) 1a. ^{15}N NMR (50.7 MHz, 10% D_2O) δ: -39.7 (with satellite peaks at -37.1 ppm and -42.3 ppm, $^1J_{Pt\text{-}N}$ = 260 Hz and $^2J_{Pt\text{-}H}$ = 53 Hz) ppm. ^{1}H NMR (500 MHz 10% D_2O) δ: 2.13 (s, 3H, CH_3), 6.11 (d with ^{195}Pt satellite peaks, $^1J_{H\text{-}15N}$ = 75 Hz, $^2J_{H\text{-}Pt}$ = 53 Hz, 6H, NH_3) ppm. ESI-MS (positive ion mode): found 378.1 (9%) and 360.1 (100%) *m/z*. Calc. for $[C_2H_{12}Cl_2N^{15}N_2O_2Pt]^+$ 378.0 $[M+H]^+$ and $[C_2H_{10}Cl_2N^{15}N_2OPt]^+$ 360.0 $[M\text{-}OH]^+$ *m/z*.

(^{15}N) 1b. ^{15}N NMR (50.7 MHz, 10% D_2O) δ: -35.7 (with ^{195}Pt satellite peaks at -33.0 ppm and -38.4 ppm, $^1J_{Pt\text{-}N}$ = 270 Hz and $^2J_{Pt\text{-}H}$ = 53 Hz) ppm; ^{1}H NMR (500 MHz; 10% D_2O) δ: 2.13 (s, 3H, CH_3), 6.06 (d with ^{195}Pt satellite peaks, $^1J_{H\text{-}15N}$ = 75 Hz, $^2J_{H\text{-}Pt}$ = 53 Hz, 6H, NH_3) ppm. ESI-MS (positive ion mode): found 379.3 (47%) and 361.2 (100%) *m/z*. Calc. for $[C_2H_{11}Cl_2{}^{15}N_2O_3Pt]^+$ 379.0 $[M+H]^+$ and $[C_2H_9Cl_2{}^{15}N_2O_2Pt]^+$ 361.0 $[M\text{-}OH]^+$ *m/z*.

X-ray structure of 3b

Crystals of **3b** suitable for single-crystal X-ray diffraction were grown by slow evaporation of aqueous solution of the complex. A specimen of size 0.6×0.4×0.4 mm, was mounted on a glass fibre and used for data collection on a SMART APEX2 diffractometer [λ(Mo-Kα) = 0.71073 Å]. The crystal is monoclinic, space group $P2_1/c$, cell parameters of a = 10.400(2), b = 10.093(2), c = 13.361(2) Å, β = 100.644(3)°, V = 1378.4(4) Å^3. The asymmetric unit is formed by two independent molecules of formula $C_6H_{17}Cl_2N_3O_3Pt$, M_r = 445.21, Z = 4, D_c = 2.14 g cm^{-3}, μ = 10.56 mm^{-1}, F(000) =840. A semi-empirical absorption correction, based on multiple scanned equivalent reflections, has been carried out and gave $0.3658 < T < 0.7459$). A total of 15205 reflections were collected up to a θ range of 29.31° (±14 *h*, ±13 *k*, ±18 *l*), 3750 unique reflections (R_{int} = 0.071). The SAINT software[15] was used for integration of reflection intensity and scaling, and SADABS[16] for absorption correction. Structures were solved by direct methods using SIR97[17] and refined by full-matrix least-squares on all F^2 using SHELXL97[18] implemented in the WinGX package.[19] All the non-hydrogen atoms in the molecules were refined anisotropically. The hydrogen atoms were partly found and partly placed in the ideal positions using riding models. CCDC 1442209 contains the supplementary crystallographic data (http://www.ccdc.cam.ac.uk/data_request/cif; see also ESI).

Theoretical calculations

DFT calculations were performed at the B3LYP level,[20, 21] with SDD core potential and basis set on Pt[22] and 6-31+G(d,p) on light atoms,[23, 24] using Gaussian09.[25] Complexes were built manually and geometry optimised without any symmetry constraint, and the resulting structures confirmed as true minima through harmonic frequency calculation. Atomic partial charges were calculated using the Natural Bond Orbital (NBO) scheme.[26] Solvation effects were accounted for by the polarizable continuum model (PCM) approach.[27]

Solution behaviour and reduction reactions

The stability of complexes of the series **a** and **b** was studied by means of ^{1}H NMR spectroscopy. The complexes ([Pt] = 20 mM, except **4a/b** and **5a/b** where saturated solutions were employed, [Pt] < 20 mM) were dissolved in 100 mM phosphate buffer (D_2O, pH 7.4) and maintained at 25 °C up to 3 d.

The reduction of complexes of the series **a** and **b** (0.5 mM) with ascorbic acid (5 mM) was studied in HEPES (2 mM, pH 7.5) at 25 °C. All these reactions were followed by monitoring the decrease of the area of the chromatographic peaks of the Pt complexes in HPLC-UV-MS. The mobile phase was a mixture of 15 mM aqueous HCOOH and CH_3OH in a ratio depending on the lipophilicity of the complex (from 90/10 to 30/70). ^{15}N NMR spectra of 20 mM solutions of Pt complexes and 40 mM ascorbic acid were recorded in 80 mM HEPES with 10% v/v D_2O at 25 °C.

Cell culture and viability tests

The compounds under investigation were tested on the human ovarian carcinoma cell line A2780, from ECACC, purchased from ICLC (Interlab Cell line Collection, IST Genova, Italy). The cells were grown in RPMI-1640 medium supplemented with L-glutamine (2 mM), penicillin (100 IU mL^{-1}), streptomycin (100 mg L^{-1}) and 10% fetal bovine serum. Cell culture and the treatments were carried on at 37 °C in a 5% CO_2 humidified chamber. Cisplatin was dissolved in 0.9% w/v NaCl aqueous solution brought to pH 3 with HCl (final stock concentration 1 mM). All Pt(IV) complexes and [Pt(acetylamido-*N*)Cl$(NH_3)_2$] were dissolved in water or absolute ethanol (final stock concentration 1-5 mM) and stored at -20 °C. The concentration was confirmed by means of ICP-OES.

The mother solutions were diluted in complete medium, to the required concentration range. In the case of co-solvent the total absolute ethanol concentration never exceeded 0.2% (this concentration was found to be non-toxic to the tested cell). Cells were treated with the compounds under investigation for 72 h. To assess the growth inhibition of the compounds under investigation, a cell viability test, i.e. the resazurin reduction assay, was used.[28] Briefly, cells were seeded in black sterile tissue-culture treated 96-well plates. At the end of the treatment, viability was assayed by 10 μg mL^{-1} resazurin (Acros Chemicals, France) in fresh medium for 1 h at 37 °C, and the amount of the reduced product, resorufin, was measured by means of fluorescence (excitation $\lambda = 535$ nm, emission $\lambda = 595$ nm) with a Tecan Infinite F200Pro plate reader (Tecan, Austria). In each experiment, cells were challenged with the drug candidates at different concentrations and the final data were calculated from at least three replicates of the same experiment performed in triplicate. The fluorescence of 8 wells containing the medium without cells was used as blank. Fluorescence data were normalized to 100% cell viability for untreated (NT) cells. Half inhibiting concentration (IC_{50}), defined as the concentration of the drug reducing cell viability by 50%, was obtained from the dose-response sigmoid using Origin Pro (version 8, Microcal Software, Inc., Northampton, MA, USA).

Cellular Pt accumulation

A2780 cells were seeded in 25 cm^2 T-flasks and treated with the complexes under investigations (10 μM) for 4 h. At the end of the exposure, cells were washed three times with phosphate buffered saline, detached from the Petri dishes using 0.05% Trypsin 1X + 2% EDTA (HyClone, Thermo Fisher) and harvested in fresh complete medium. An automatic cell counting device (Countess®, Life Technologies), was used to measure the number and the mean diameter from every cell count. From the same sample, about 5×10^6 cells were taken out for cellular accumulation analysis. Moreover, 100 μL of medium were taken out from each sample at time zero to check the extracellular Pt concentration. For the cellular Pt accumulation analysis, the cells were transferred into a borosilicate glass tube and centrifuged at 1100 rpm for 5 min at room temperature. The supernatant was carefully removed by aspiration, while about 200 μL of the supernatant were left in order to limit the cellular loss. Cellular pellets were stored at -20 °C until mineralization. Platinum content determination was performed by ICP-MS (Thermo Optek X Series 2). Instrumental settings were optimized in order to yield maximum sensitivity for platinum. For quantitative determination, the most abundant isotopes of platinum and indium (used as internal standard) were measured at *m/z* 195 and 115, respectively. Mineralization was performed by addition of 70% w/w HNO_3 to each sample (after defrosting), followed by incubation for 1 h at 60 °C in an ultrasonic bath. Before the ICP-MS measurement, the HNO_3 was diluted to a final 1% concentration. The cellular Pt accumulation was referred as ng Pt per 10^6 cells. In order to obtain the Pt cellular concentration, the total cellular volume of each sample was obtained considering the mean cell diameter and cell number estimated by means of an automatic cell counting device (Countess®, Life Technologies). The ratio between the internal and the external cell Pt concentration, namely, the Accumulation Ratio (AR) was computed as previously reported.[29]

Results and Discussion

Synthesis of 1a-5a and 1b-5b and X-ray structure of 3a

Complex **1a** has been synthesized upon oxidation of cisplatin with hydrogen peroxide in a mixture of acetonitrile and methanol, according to a recently reported method.[9] During this reaction the reactive intermediate PAIA (Scheme 1) provides a hydroxide and an acetylamido ligand, the latter being N-coordinated during the Pt(II)→Pt(IV) oxidation step. The peroxide PAIA has a quite unstable oxygen-oxygen bond,[30] which should easily split into reactive radicals (namely $^{\bullet}OH$ and $^{\bullet}OC(=NH)CH_3$) via homolytic cleavage able to coordinate to Pt during its oxidation from II to IV redox state. ESR measurements, performed on the reaction mixture using 5,5-dimethyl-1-pyrroline-*N*-oxide (DMPO) as spin trap, confirm the formation of radical species. However, the presence of several solvents (in particular acetonitrile and methanol that can react with H_2O_2 and change the coupling constants) makes the interpretation of the spectra doubtful.

Interestingly, the final product **1a** has the acetylamido fragment N-coordinated. The mesomeric transformation from O-bonded to N-bonded acetylamido is justified considering the relative stability of the two possible complexes. In spite of its high oxidation state, Pt(IV) is classified as a soft ion in the Pearson's HSAB theory, and therefore it should prefer N-over O-coordination.[31] Moreover, the ground state energy evaluated for both the isomeric complexes by means of DFT calculations give free energy difference of 55.8 kJ mol^{-1} in favour of the N-coordinated over O-coordinated form.

Complex **1b** was obtained from the oxidation of cisplatin with hydrogen peroxide in acetic acid according a slight modification of a previously reported procedure (Scheme 2).[13] These two compounds were reacted with the different anhydrides, to obtain the axially asymmetric complexes **2a/b-4a/b**, or with activated n-octanoic acid, to obtain **5a** and **5b**. The reaction of **1a** with anhydrides/octanoic acid did not modify the arrangement of the coordinating atoms around the Pt centre (i.e. the cisplatin arrangement), as testified by the NMR data. In fact, all complexes of the **a** series show a ^{195}Pt NMR chemical shift similar to that of the prototype **1a**, in the 400-500 ppm region (for series **b** ^{195}Pt NMR chemical shift falls in the 1000-1250 region).

The X-ray structure of **3a**, represented in the ORTEP view of Fig. 1, confirms the presence of a "N_3Cl_2O" arrangement around the Pt atom. The coordination geometry of Pt(IV) is octahedral with the equatorial plane occupied by the two chlorido ligands [Pt–Cl1 2.325(2) and Pt–Cl2 2.314(2) Å] and the two ammonia molecules [Pt–N1 2.052(6) and Pt–N2 2.036(5) Å]. The octahedral coordination is completed by the acetylamido ligand, which occupies one apical position through the deprotonated amino group (Pt-N3 1.987(7) Å), and the butanoato, through the deprotonated OH group (Pt-O2 2.039(6) Å). The arrangement of the axial ligands is very close to linearity (N3-Pt1-O2 175.6(2)°).

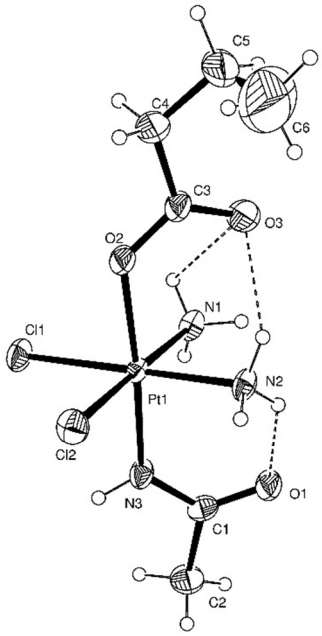

Fig. 1. ORTEP representation of **3a** with ellipsoids at 50% probability (intramolecular hydrogen bonds are represented with dashed lines).

The orientation of the butanoato ligand is mainly due to bifurcated hydrogen bond between its carbonyl and both ammonia molecules. The hydrophobic tail showed a certain degree of disorder and had to be constrained in the refinement. In complex **1a**,[9] the carboxylate plane almost bisected the N-Pt-N angle (47.83°) forming two hydrogen bonds with both ammines, while in this molecule, the acetylamido oxygen is involved in only one intramolecular hydrogen bond with N2 (the corresponding angle is 54.71°). In addition, O1 also forms two intermolecular hydrogen bonds with both ammines of an adjacent centrosymmetrical complex (Fig. 2). Thanks to these latter bonds, the molecules interact pairwise, head-to-tail, forming dimer-like units. These dimeric units are in turn interconnected with each other through another set of hydrogen bonds that involves the butanoate oxygen coordinated to the platinum.

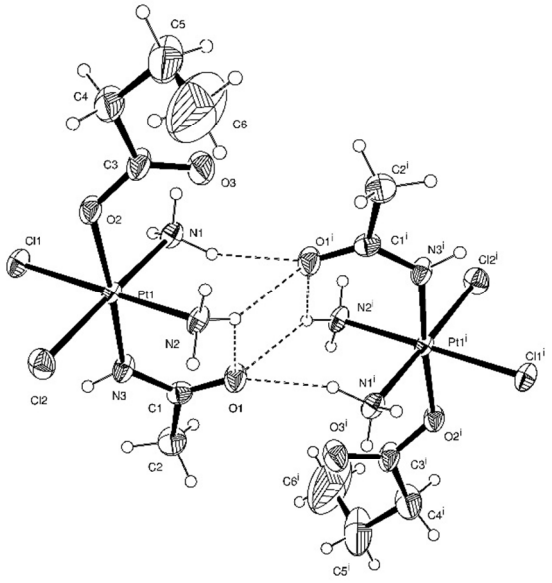

Fig. 2. Scheme of intermolecular hydrogen bonds which bring to the formation of dimer-like units of two centrosymmetrically related molecules (i = 1-x, 1-y, 1-z).

Comparing this molecule with similar ones reported in the literature[32-34] it is possible to observe a common feature that characterises these structures. When the two equatorial ammines are free to rotate around the Pt-N axis, the oxygen atom of the carbonyl moiety belonging to the ligand in one of the two axial positions forms a strong bifurcated hydrogen bond with them, orienting their hydrogens. On the opposite site of the coordination plane, the corresponding carbonyl group cannot find ammine hydrogens suitably oriented to form analogous hydrogen bonds and therefore this second carboxyl group is free to rotate around the Pt-O bond and orient itself to form other interactions with neighbouring molecules. In systems in which the ammine groups are part of a more complex molecule,[35] and therefore constrained to certain orientations, the intramolecular hydrogen bonds cannot form and the carboxyl groups are free and involved in single intra- and inter-molecular bonds. To complete the network of interactions that holds together the crystal, a further hydrogen bond is found between O2 and N2 of an adjacent molecule (-x+1, +y+1/2, -z+1/2) which creates a planar network extending parallel to the *(100)* plane of the unit cell. The hydrophobic tails of the butanoato chains are exposed on both sides of the plane. The whole structure is then completed by van der Waals interactions between the hydrophobic surfaces of these planes (see Fig. S1, ESI).

Solution behaviour and reduction reactions

The complexes of the two series were kept in phosphate buffer (100 mM in D_2O, pH = 7.4) for 3 d at 37 °C, and the solutions were analysed by means of ^1H NMR spectroscopy. The results show that the acetylamido complexes (series **a**) are stable, both when maintained in the dark and exposed to natural daylight cycles (Figs. S2-S6, ESI), whereas for series **b** the exposition to light influences the solution behaviour (Figs. S7-S13, ESI). In

fact, all compounds **1b**-**5b** are stable in the dark (*i.e.*, no variation in the axial acetato ^{1}H NMR peak intensity, taken as diagnostic signal), in the time interval considered (3 d). In contrast, the methyl signal of **1b** and **2b** decreases with time when the solution is not kept in the dark. After 24 h, the C*H*$_3$ peaks of the coordinated acetato ligand decreased by 10 and 20%, for **1b** and **2b**, respectively. At the same time, an increase of the free acetato signal was observed. ^{195}Pt NMR of the aged solutions did not show peaks belonging to Pt(II) derivatives, confirming that hydrolysis, rather than reduction, occurred. It is generally believed that Pt(IV) compounds are quite inert to ligand substitution reaction; however, it has been reported that aquation reaction may occur to some extent,[36] in particular after exposure to light or in the presence of residual Pt(II) "impurities" that act as catalysts.[14]

The complexes under investigation were reacted with ascorbic acid (AA) as the simplest model of bio-reductant in order to verify the reduction kinetics and, more importantly, to identify the produced metabolites. All measurements were performed with a 10-fold excess of AA in HEPES buffer, monitoring the decrease of the area of the Pt(IV) HPLC peak. The hydroxido complexes **1a** and **1b** showed significant decrease of the HPLC peak area (after 24 h **1a** and **1b** showed a decrease in peak area of about 45% and 60%, respectively) (Figs. S14 and S19, ESI). On the contrary, for all the remaining complexes **2**-**5**/**a**-**b** only a 0-15% of peak decrease was observed in the same timescale (Figs. S5-S18 and S20-S23, ESI). This is in agreement with the previous observation that OH ligands favour the kinetics of Pt(IV) reduction over the carboxylato ligands.[37]

As far as the reduction is concerned, the usual Pt(II) metabolites deriving from the reductive elimination of the axial ligands (*i.e.*, cisplatin and its hydrolysed derivatives) were observed in both series.[1, 11] Interestingly, the reduction process of complexes **a** is accompanied also by the formation of a low quantity of *cis*-[Pt(acetylamido-*N*)Cl(NH$_3$)$_2$] (Fig. S24, ESI; ESI-MS shows this complex along with some hydrolyzed species) (Scheme 3).

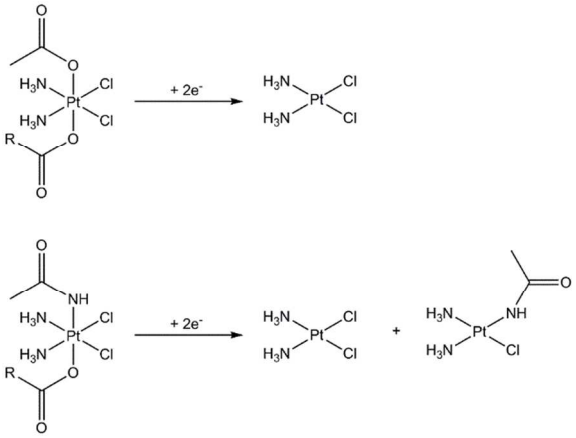

Scheme 3. General reduction scheme of complexes **a** and **b**. Hydrolyzed products and organic residues were omitted for clarity.

To confirm these observations, reduction with AA was performed on **1a** and **1b** bearing ^{15}N ammonia[14] as equatorial ligands and followed by ^{15}N NMR (twice excess of AA in HEPES buffer; Figs. S25-S26, ESI). After 1 h, the [^{1}H, ^{15}N] HSQC spectra showed the presence of the signals of residual **1a** (^{15}NH$_3$ δ = -39.7 ppm with satellite peaks at -37.1 ppm e -42.3 ppm, $^1J_{Pt\text{-}N}$ = 258 Hz and $^2J_{Pt\text{-}H}$ = 53 Hz; ^{1}H δ = 6.11 ppm) or **1b** (^{15}NH$_3$ δ = -35.7 ppm with satellite peaks at -33.0 ppm e -38.4 ppm, $^1J_{Pt\text{-}N}$ = 270 Hz and $^2J_{Pt\text{-}H}$ = 53 Hz; ^{1}H δ = 6.06 ppm), together with that of cisplatin (^{15}NH$_3$ δ = -66.8 ppm with satellite peaks at -63.5 ppm e -69.9 ppm, $^1J_{Pt\text{-}N}$ = 327 Hz and $^2J_{Pt\text{-}H}$ = 69 Hz; ^{1}H δ = 4.10 ppm). As expected, the signal of cisplatin decreased with time and new peaks appeared at δ = -65.0 ppm (^{1}H δ = 4.33 ppm) and -88.0 ppm (^{1}H δ = 4.25 ppm), respectively. The latter signal falls in the typical region for ^{15}N *trans* to oxygens, supporting the formation of hydrolysed cisplatin.[38]

In the case of **1a**, another peak was present at ^{15}NH$_3$ δ = -69.0 ppm (^{1}H δ = 4.33 ppm), in a region common to ^{15}N *trans* to chloridos or nitrogens, compatible with the formation of *cis*-[Pt(acetylamido-*N*)Cl(^{15}NH$_3$)$_2$]. Moreover, over time, some other peaks appeared in the region for ^{15}N *trans* to oxygens, indicating the formation of various new hydrolysed species. ^{195}Pt NMR on the same solution showed signals of cisplatin and its hydrolysed derivative, along with another peak at -2338 ppm (Fig. S27, ESI). A genuine sample of *cis*-[Pt(acetylamido-*N*)Cl(NH$_3$)$_2$][12] showed almost the same ^{195}Pt chemical shift (δ = -2328 ppm in D$_2$O). Therefore, the combination of NMR and MS information strengthen the hypothesis of the formation of *cis*-[Pt(acetylamido-*N*)Cl(NH$_3$)$_2$] as by-product of the reduction of Pt(IV)-acetylamido complexes.

The scrambling between an equatorial chlorido and an axial acetato ligand is not unusual, as clearly showed by Gibson et al. following the reduction of a number of Pt(IV) derivatives.[1] The resulting mixed chlorido/carboxylato Pt(II) metabolite should retain the original antiproliferative activity, since Keppler et al. demonstrated that monodentate carboxylato ligands bounded to Pt(II) complexes are able to undergo efficient activation by aquation.[39] The faster the aquation, the faster the coordination to DNA and the higher the activity. On the contrary, the scrambling between an equatorial chlorido and the axial acetylamido ligand, partially occurring during the reduction of **1a,** causes a decrease in the activity of the resulting Pt(II) metabolite, since the N-acetylamido ligand cannot undergo easily hydrolysis (see below).

The redox properties of the two series of compounds were tested by linear sweep voltammetry in ethanol solution. All complexes showed the usual Pt(IV)-electrochemical behaviour: a chemically irreversible 2e$^-$, broad reduction peak was observed corresponding to the loss of the two axial ligands and the change from octahedral Pt(IV) to square-planar Pt(II) species.[40] The reduction peak potentials, E_p, of complexes **a** and **b**, reveal that the acetylamido complexes are reduced at a more cathodic potential (ΔE_p = 0.165 V as average difference between the two **a** and **b** series; Table S3, ESI). The *N*-coordinated acetylamido provides more electronic density on the Pt centre than the acetato counterpart, making the related **a** series (thermodynamically) less easily reducible. This is supported by DFT calculations, from which the atomic partial charge on Pt, calculated using the Natural Bond Orbital (NBO) scheme,[26] in acetato complex is predicted to be +0.574, compared to that in acetylamido of +0.503. This suggests that N-coordination does indeed donate more electron density to Pt than O.

It has been previously reported for cisplatin-, nedaplatin-,

picoplatin-, and oxaliplatin-based Pt(IV) complexes that E_p values measured in water increase (becomes less negative) as the axial chain length increases.[33, 41, 42] On the contrary, it has been observed that in organic solvent Pt(IV) complexes with different axial chains show very similar E_p values, pointing out that the chain length of the carboxylato ligand has no influence at all on the electronic characteristics of the Pt centre, and, hence, on the reduction potential.[43] In water different solvation effects on the species involved in the reduction mechanism do influence the final E_p value. The complexes under investigation confirm the latter observation: E_p values measured in pure ethanol are very similar within each series; unfortunately no well-defined reduction peaks could be observed in water to corroborate the former statement.

Antiproliferative activity

The acetylamido complexes **2a**-**5a** were tested on ovarian A2780 tumor cells, together with their acetato counterparts **2b**-**5b**, cisplatin, and *cis*-[Pt(acetylamido-*N*)Cl(NH_3)$_2$] for comparison purposes. The results are expressed in terms of IC_{50} (half-maximal inhibitory concentration) and are reported in Fig. 3 (see also Table S3, ESI).

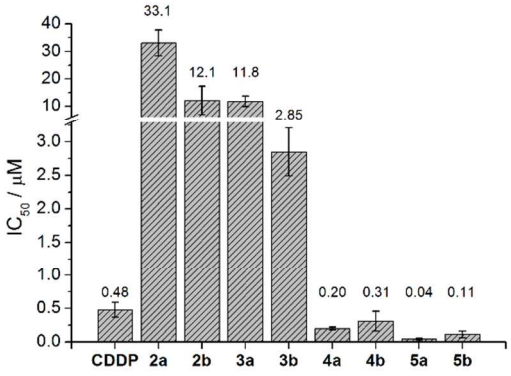

Fig. 3. Half-inhibitory concentration of cisplatin (CDDP), complexes **2a**-**5a**, and complexes **2b**-**5b**, measured on A2780 ovarian cancer cells treated for 72 h with the compounds.

It has been reported that Pt(IV) complexes enter cells by passive diffusion only, and unlike cisplatin no influx/efflux mechanism appears to operate.[29] For this reason, lipophilicity, directly related to the ability of a molecule to passively cross cellular membranes, is a key feature to determine the biological activity of such complexes. Lipophilicity of the complexes under investigation was evaluated by means of HPLC, since retention is due to partitioning between C18 chains of the stationary phase (representing the cellular membrane) and aqueous eluent (representing the water inside and outside cells)[33, 44] (Table S3, ESI). The data show that the retention is minimally affected by the presence of coordinated axial acetato (series **b**) instead of acetylamido (series **a**), whereas it depends mainly on the second axial ligand. As expected, this similarity is reflected on the accumulation ratio (AR) of the **2**-**5** pairs (Fig. 4, see also Table S3, ESI). In the literature, uptake and accumulation of Pt are sometimes used as synonymous, but actually the AR is the quotient between the internal and the external cellular Pt concentration. The (internal) cellular Pt concentration is measured taking into account the experimentally measured cell number and average volume of cells, the external Pt concentration is that in the culture medium (experimentally verified by ICP-MS).

On the contrary, the acetato complexes **b** show better antiproliferative activity with respect to acetylamido complexes **a** when the companion carboxylato exhibits shorter chains (**2b** and **3b** vs. **2a** and **3a**). As the carboxylato ligand chain extends, antiproliferative activities became quite similar (**4b** and **5b** vs. **4a** and **5a**) to the acetylamido ones, matching their similar cell uptake. The difference between **2b-3b** and **2a-3a** may be ascribed to the different kinetics of reduction: the acetato series **b** is more prone to reduction than series **a**. Moreover, both series produce cisplatin as the major metabolite, but series **a** produces also moderate (about 5% in the abiological conditions employed in the reduction experiments with AA) amount of *cis*-[Pt(acetylamido-*N*)Cl(NH_3)$_2$], which is about 50 times less active than cisplatin (IC_{50} = 24.5 µM, measured from a genuine sample). It is well known that monofunctional Pt(II)-triamine complexes such as [PtCl(NH_3)$_3$]$^+$ have lower activity than bifunctional ones, unless they have a bulky amine, such as phenanthriplatin.[45-48] Thus, the formation of the [Pt(acetylamido-*N*)Cl(NH_3)$_2$] metabolite is detriment for the overall antiproliferative activity. However, the higher lipophilicity imparted by long chains (**4b-5b** and **4a-5a**) makes the cell uptake so high to mitigate the above differences. Finally, inside each series, the usual relationship is observed: higher lipophilicity corresponds to lower IC_{50}.[42]

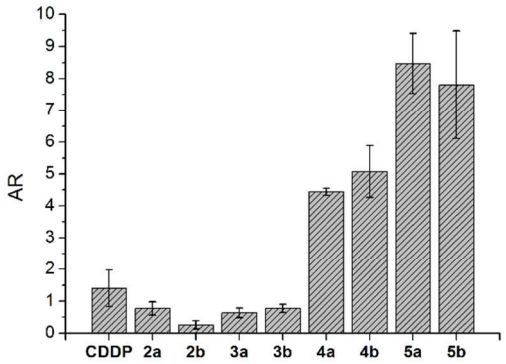

Fig. 4. Accumulation ratio of cisplatin (CDDP), complexes **2a**-**5a**, and complexes **2b**-**5b**, measured on A2780 ovarian cancer cells treated for 4 h with the compounds.

Conclusions

A series (**a**) of cisplatin-based, asymmetric Pt(IV) complexes of general formula [Pt(acetylamido-*N*)($CH_3(CH_2)_nCOO$)Cl$_2$(NH_3)$_2$] (n = 0, 2, 4, 6), bearing an acetylamido axial ligand were synthesized and their antiproliferative potential was evaluated. Their cytotoxic activity was investigated in A2780 ovarian cancer cell line showing IC_{50} values in the low µM range. This antiproliferative activity is similar to or somewhat lower than that of the corresponding acetato series (**b**) [Pt(acetato)($CH_3(CH_2)_nCOO$)Cl$_2$(NH_3)$_2$] (n = 0, 2, 4, and 6) depending on n.

Interestingly, starting from n = 2, IC_{50} values are similar to that of the prototype metallo-drug cisplatin. Compounds of series **a** can be obtained easily and in high yield, exhibit an optimal lipophilicity/aqueous solubility balance, and have good stability under light, thus they represent an interesting and promising class of potential antitumor prodrugs.

Acknowledgments

We are indebted to Compagnia di San Paolo (Torino, Italy) for the financial support to the research project BIPLANES. Inter-University Consortium for Research on the Chemistry of Metals in Biological Systems (CIRCMSB, Bari, Italy), and UE-COST CM1105 Action "Functional metal complexes that bind to biomolecules" are also acknowledged for providing opportunities of stimulating discussions and short term missions. JAP acknowledges use of ARCCA (Advanced Research Computing @ Cardiff) facilities for DFT studies.

Notes and references

[a] *Dipartimento di Scienze e Innovazione Tecnologica, Università del Piemonte Orientale, Viale Teresa Michel 11, 15121 Alessandria (Italy). Fax: +39 0131 360250; Tel: +39 0131 360266; E-mail: domenico.osella@uniupo.it*

[b] *Dipartimento di Chimica, Università di Parma, Parco Area delle Scienze, 17/A, 43124 Parma (Italy).*

[c] *School of Chemistry, Cardiff University, Park Place, Cardiff CF10 3AT (United Kingdom)*

† Electronic supplementary information (ESI) available: X-ray, water solubility values, redox potentials, HPLC retention times, stability and reduction data of the complexes under investigation. For ESI and crystallographic data in CIF format see DOI: 10.1039/…

1. E. Wexselblatt and D. Gibson, *Journal of Inorganic Biochemistry*, 2012, **117**, 220-229.
2. M. D. Hall, H. R. Mellor, R. Callaghan and T. W. Hambley, *Journal of Medicinal Chemistry*, 2007, **50**, 3403-3411.
3. C. F. Chin, D. Y. Q. Wong, R. Jothibasu and W. H. Ang, *Current Topics in Medicinal Chemistry*, 2011, **11**, 2602-2612.
4. E. Gabano, M. Ravera and D. Osella, *Current Medicinal Chemistry*, 2009, **16**, 4544-4580.
5. J. S. Butler and P. J. Sadler, *Current Opinion in Chemical Biology*, 2013, **17**, 175-188.
6. X. Wang, X. Wang and Z. Guo, *Accounts of Chemical Research*, 2015, **48**, 2622-2631.
7. M. Ravera, E. Perin, E. Gabano, I. Zanellato, G. Panzarasa, K. Sparnacci, M. Laus and D. Osella, *Journal of Inorganic Biochemistry*, 2015, **151**, 132-142.
8. M. Ravera, E. Gabano, G. Pelosi, F. Fregonese, S. Tinello and D. Osella, *Inorganic Chemistry*, 2014, **53**, 9326-9335.
9. G. Pelosi, M. Ravera, E. Gabano, F. Fregonese and D. Osella, *Chemical Communications (Cambridge, England)*, 2015, **51**, 8051-8053.
10. S. C. Dhara, *Indian Journal of Chemistry*, 1970, **8**, 193-194.
11. I. Zanellato, I. Bonarrigo, D. Colangelo, E. Gabano, M. Ravera, M. Alessio and D. Osella, *Journal of Inorganic Biochemistry*, 2014, **140**, 219-227.
12. A. Erxleben, I. Mutikainen and B. Lippert, *Journal of the Chemical Society-Dalton Transactions*, 1994, 3667-3675.
13. J. Z. Zhang, P. Bonnitcha, E. Wexselblatt, A. V. Klein, Y. Najajreh, D. Gibson and T. W. Hambley, *Chemistry-a European Journal*, 2013, **19**, 1672-1676.
14. M. S. Davies, M. D. Hall, S. J. Berners-Price and T. W. Hambley, *Inorganic Chemistry*, 2008, **47**, 7673-7680.
15. SAINT: SAX, Area Detector Integration, Siemens Analytical Instruments Inc., Madison WI, USA, 1995.
16. G. M. Sheldrick, SADABS: Siemens Area Detector Absorption Correction Software, University of Göttingen, Göttingen, Germany, 1996.
17. A. Altomare, M. C. Burla, M. Camalli, G. L. Cascarano, C. Giacovazzo, A. Guagliardi, A. G. G. Moliterni, G. Polidori and R. Spagna, *Journal of Applied Crystallography*, 1999, **32**, 115-119.
18. G. M. Sheldrick, *Acta Crystallographica Section A*, 2008, **64**, 112-122.
19. L. Farrugia, *Journal of Applied Crystallography*, 1999, **32**, 837-838.
20. A. D. Becke, *Journal of Chemical Physics*, 1993, **98**, 5648-5652.
21. C. Lee, W. Yang and R. G. Parr, *Physical Review B*, 1988, **37**, 785-789.
22. D. Andrae, U. Haussermann, M. Dolg, H. Stoll and H. Preuss, *Theoretica Chimica Acta*, 1990, **77**, 123-141.
23. R. Ditchfield, W. J. Hehre and J. A. Pople, *The Journal of Chemical Physics*, 1971, **54**, 724-728.
24. T. Clark, J. Chandrasekhar, G. W. Spitznagel and P. V. R. Schleyer, *Journal of Computational Chemistry*, 1983, **4**, 294-301.
25. M. J. Frisch, G. W. Trucks, H. B. Schlegel, G. E. Scuseria, M. A. Robb, J. R. Cheeseman, G. Scalmani, V. Barone, B. Mennucci, G. A. Petersson, H. Nakatsuji, M. Caricato, X. Li, H. P. Hratchian, A. F. Izmaylov, J. Bloino, G. Zheng, J. L. Sonnenberg, M. Hada, M. Ehara, K. Toyota, R. Fukuda, J. Hasegawa, M. Ishida, T. Nakajima, Y. Honda, O. Kitao, H. Nakai, T. Vreven, J. A. Montgomery Jr., J. E. Peralta, F. Ogliaro, M. J. Bearpark, J. Heyd, E. N. Brothers, K. N. Kudin, V. N. Staroverov, R. Kobayashi, J. Normand, K. Raghavachari, A. P. Rendell, J. C. Burant, S. S. Iyengar, J. Tomasi, M. Cossi, N. Rega, N. J. Millam, M. Klene, J. E. Knox, J. B. Cross, V. Bakken, C. Adamo, J. Jaramillo, R. Gomperts, R. E. Stratmann, O. Yazyev, A. J. Austin, R. Cammi, C. Pomelli, J. W. Ochterski, R. L. Martin, K. Morokuma, V. G. Zakrzewski, G. A. Voth, P. Salvador, J. J. Dannenberg, S. Dapprich, A. D. Daniels, Ö. Farkas, J. B. Foresman, J. V. Ortiz, J. Cioslowski and D. J. Fox, Gaussian 09, Revision D.01, Gaussian, Inc., Wallingford CT, 2009.
26. A. E. Reed, R. B. Weinstock and F. Weinhold, *The Journal of Chemical Physics*, 1985, **83**, 735-746.
27. J. Tomasi, B. Mennucci and R. Cammi, *Chemical Reviews*, 2005, **105**, 2999-3093.
28. E. Magnani and E. Bettini, *Brain Research Protocols*, 2000, **5**, 266-272.
29. M. Ravera, E. Gabano, I. Zanellato, B. Ilaria, M. Alessio, F. Arnesano, A. Galliani, G. Natile and D. Osella, *Journal of Inorganic Biochemistry*, 2015, **150**, 1-8.
30. R. Benassi and E. Taddei, *Tetrahedron*, 1994, **50**, 4795-4810.
31. S. J. Lippard and J. M. Berg, *Principles of Bioinorganic Chemistry*, University Science Books, 1994.
32. S. Dhar, F. X. Gu, R. Langer, O. C. Farokhzad and S. J. Lippard, *Proceedings of the National Academy of Sciences of the United States of America*, 2008, **105**, 17356-17361.
33. J. A. Platts, G. Ermondi, G. Caron, M. Ravera, E. Gabano, L. Gaviglio, G. Pelosi and D. Osella, *Journal of Biological Inorganic Chemistry*, 2011, **16**, 361-372.
34. M. Ravera, E. Gabano, S. Bianco, G. Ermondi, G. Caron, M. Vallaro, G. Pelosi, I. Zanellato, I. Bonarrigo, C. Cassino and D. Osella, *Inorganica Chimica Acta*, 2015, **432**, 115-127.
35. V. Gandin, C. Marzano, G. Pelosi, M. Ravera, E. Gabano and D. Osella, *Chemmedchem*, 2014, **9**, 1299-1305.
36. E. Wexselblatt, E. Yavin and D. Gibson, *Angewandte Chemie-International Edition*, 2013, **52**, 6059-6062.
37. J. Z. Zhang, E. Wexselblatt, T. W. Hambley and D. Gibson, *Chemical Communications*, 2012, **48**, 847-849.
38. L. Ronconi and P. J. Sadler, *Coordination Chemistry Reviews*, 2008, **252**, 2239-2277.
39. D. Hofer, H. P. Varbanov, A. Legin, M. A. Jakupec, A. Roller, M. Galanski and B. K. Keppler, *Journal of Inorganic Biochemistry*, 2015, **153**, 259-271.
40. E. Reisner, V. B. Arion, B. K. Keppler and A. J. L. Pombeiro, *Inorganica Chimica Acta*, 2008, **361**, 1569-1583.
41. M. Ravera, E. Gabano, I. Zanellato, I. Bonarrigo, E. Escribano, V. Moreno, M. Font-Bardia, T. Calvet and D. Osella, *Dalton Transactions*, 2012, **41**, 3313-3320.

42. P. Gramatica, E. Papa, M. Luini, E. Monti, M. B. Gariboldi, M. Ravera, E. Gabano, L. Gaviglio and D. Osella, *Journal of Biological Inorganic Chemistry*, 2010, **15**, 1157-1169.
43. M. R. Reithofer, A. K. Bytzek, S. M. Valiahdi, C. R. Kowol, M. Groessl, C. G. Hartinger, M. A. Jakupec, M. Galanski and B. K. Keppler, *Journal of Inorganic Biochemistry*, 2011, **105**, 46-51.
44. G. Ermondi, G. Caron, M. Ravera, E. Gabano, S. Bianco, J. A. Platts and D. Osella, *Dalton Transactions*, 2013, **42**, 3482-3489.
45. L. S. Hollis, W. I. Sundquist, J. N. Burstyn, W. J. Heigerbernays, S. F. Bellon, K. J. Ahmed, A. R. Amundsen, E. W. Stern and S. J. Lippard, *Cancer Research*, 1991, **51**, 1866-1875.
46. L. S. Hollis, A. R. Amundsen and E. W. Stern, *Journal of Medicinal Chemistry*, 1989, **32**, 128-136.
47. K. S. Lovejoy, R. C. Todd, S. Z. Zhang, M. S. McCormick, J. A. D'Aquino, J. T. Reardon, A. Sancar, K. M. Giacomini and S. J. Lippard, *Proceedings of the National Academy of Sciences of the United States of America*, 2008, **105**, 8902-8907.
48. C. Francisco, S. Gama, F. Mendes, F. Marques, I. C. dos Santos, A. Paulo, I. Santos, J. Coimbra, E. Gabano and M. Ravera, *Dalton Transactions*, 2011, **40**, 5781-5792.

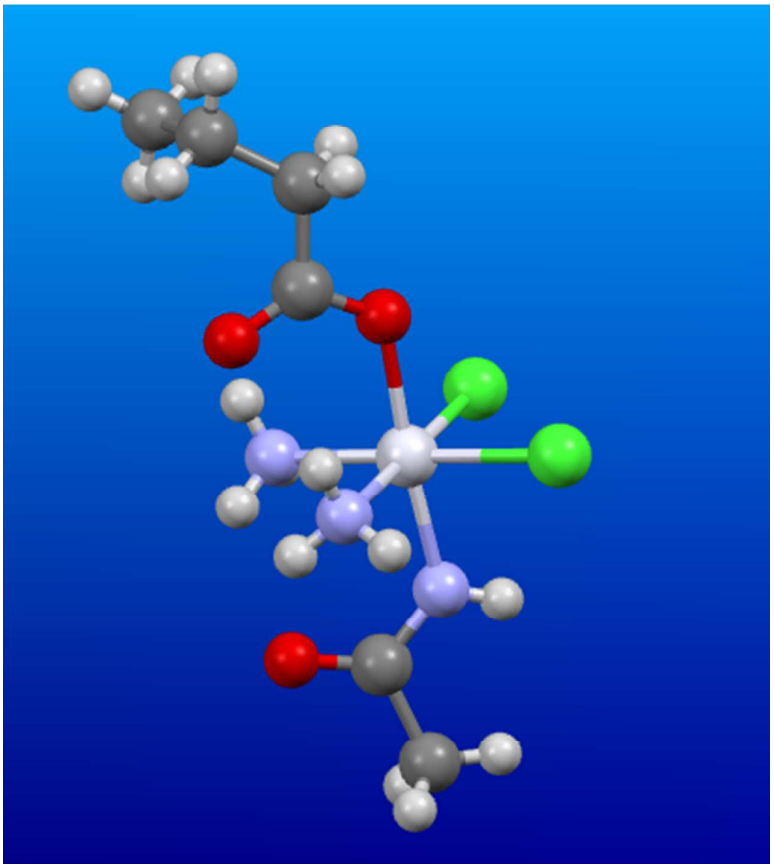

The synthesis and biological properties of Pt(IV) complexes exhibiting an asymmetric combination of axial acetylamido and carboxylato ligands are reported.

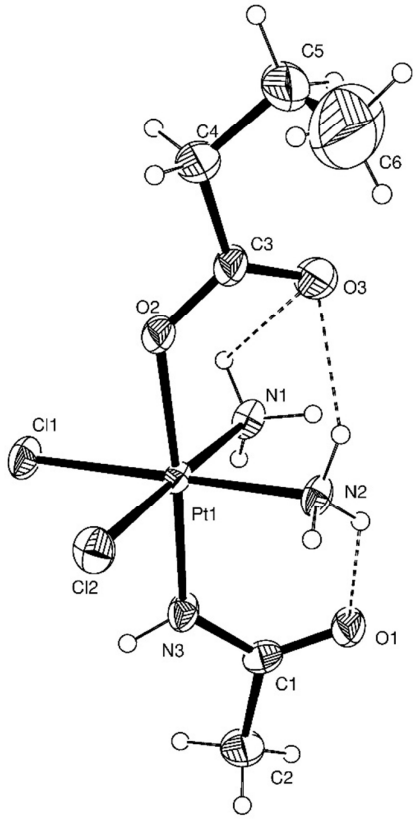

Fig. 1. ORTEP representation of **3a** with ellipsoids at 50% probability (intramolecular hydrogen bonds are represented with dashed lines).

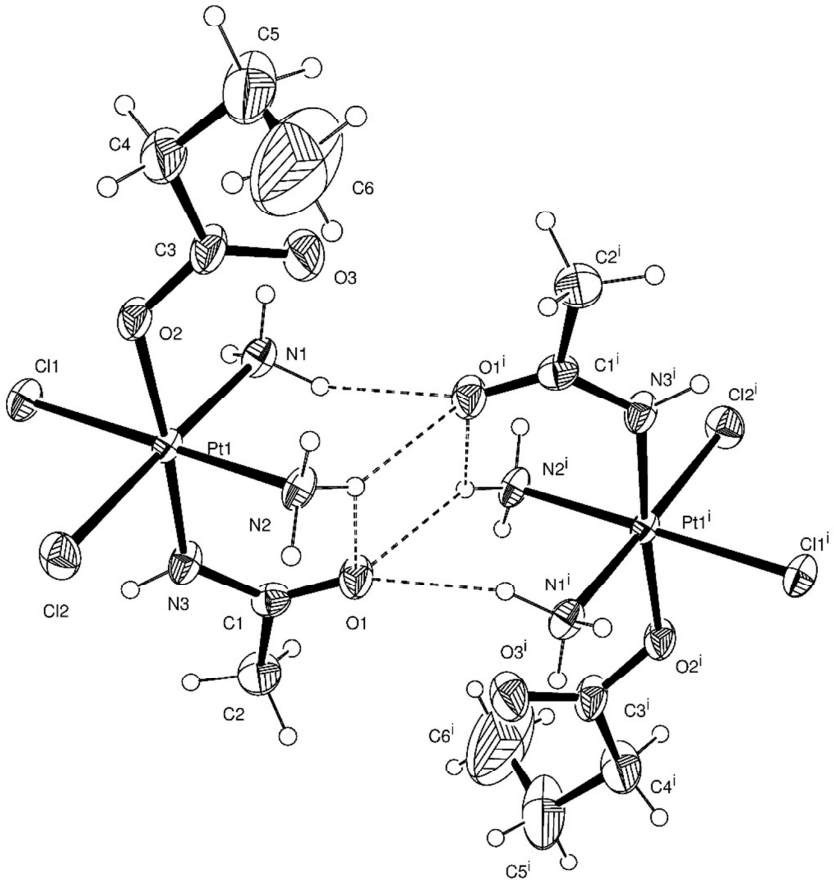

Fig. 2. Scheme of intermolecular hydrogen bonds which bring to the formation of dimer-like units of two centrosymmetrically related molecules (i = 1-x, 1-y, 1-z).

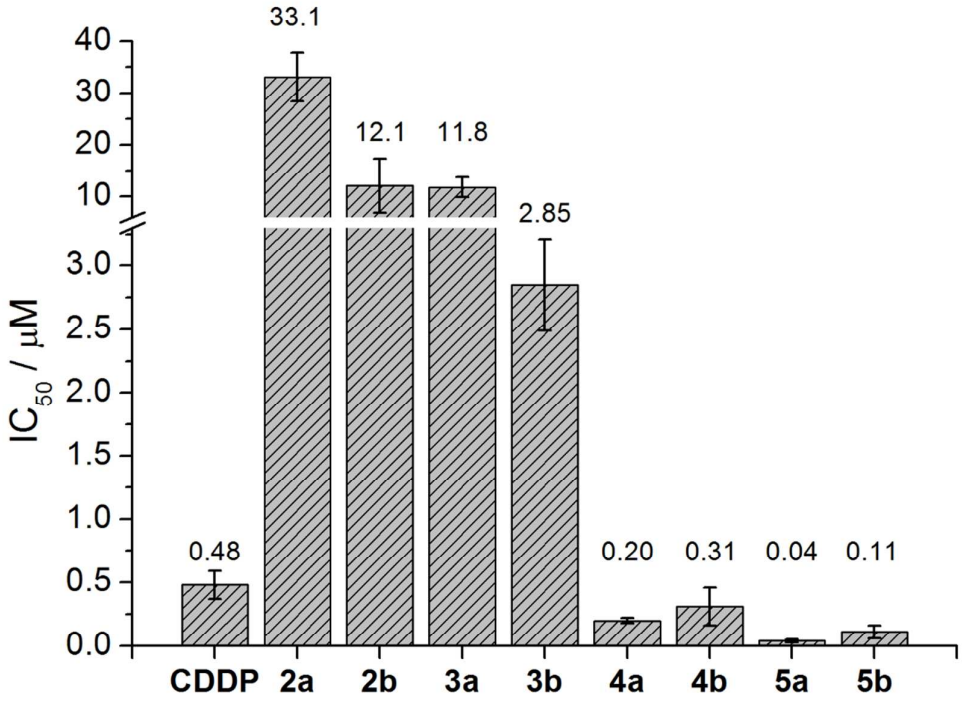

Fig. 3. Half-inhibitory concentration of cisplatin (CDDP), complexes **2a**-**5a**, and complexes **2b**-**5b**, measured on A2780 ovarian cancer cells treated for 72 h with the compounds.

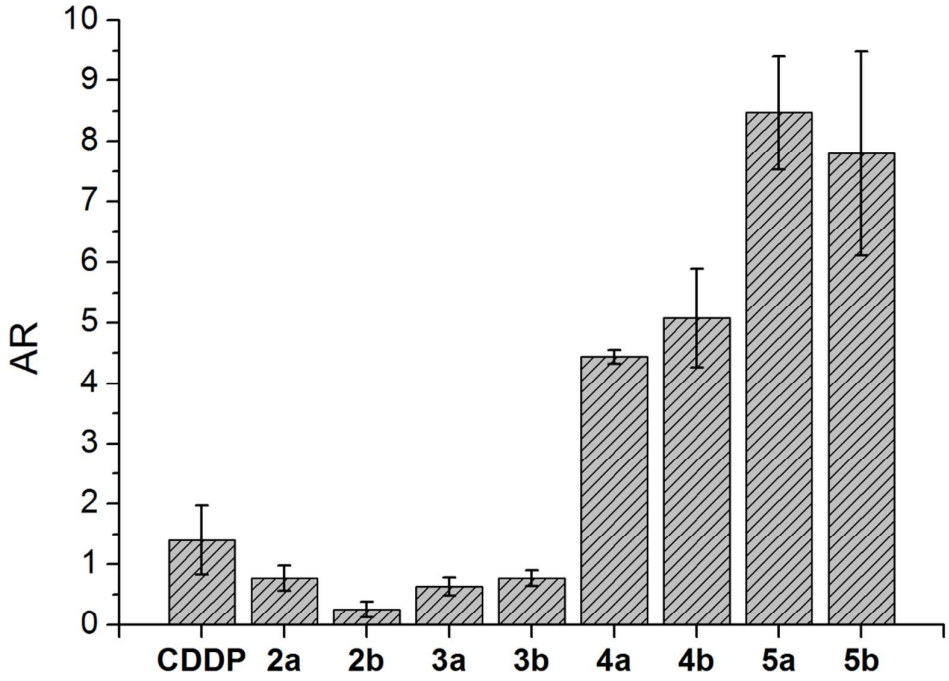

Fig. 4. Accumulation ratio of cisplatin (CDDP), complexes **2a**-**5a**, and complexes **2b**-**5b**, measured on A2780 ovarian cancer cells treated for 4 h with the compounds.

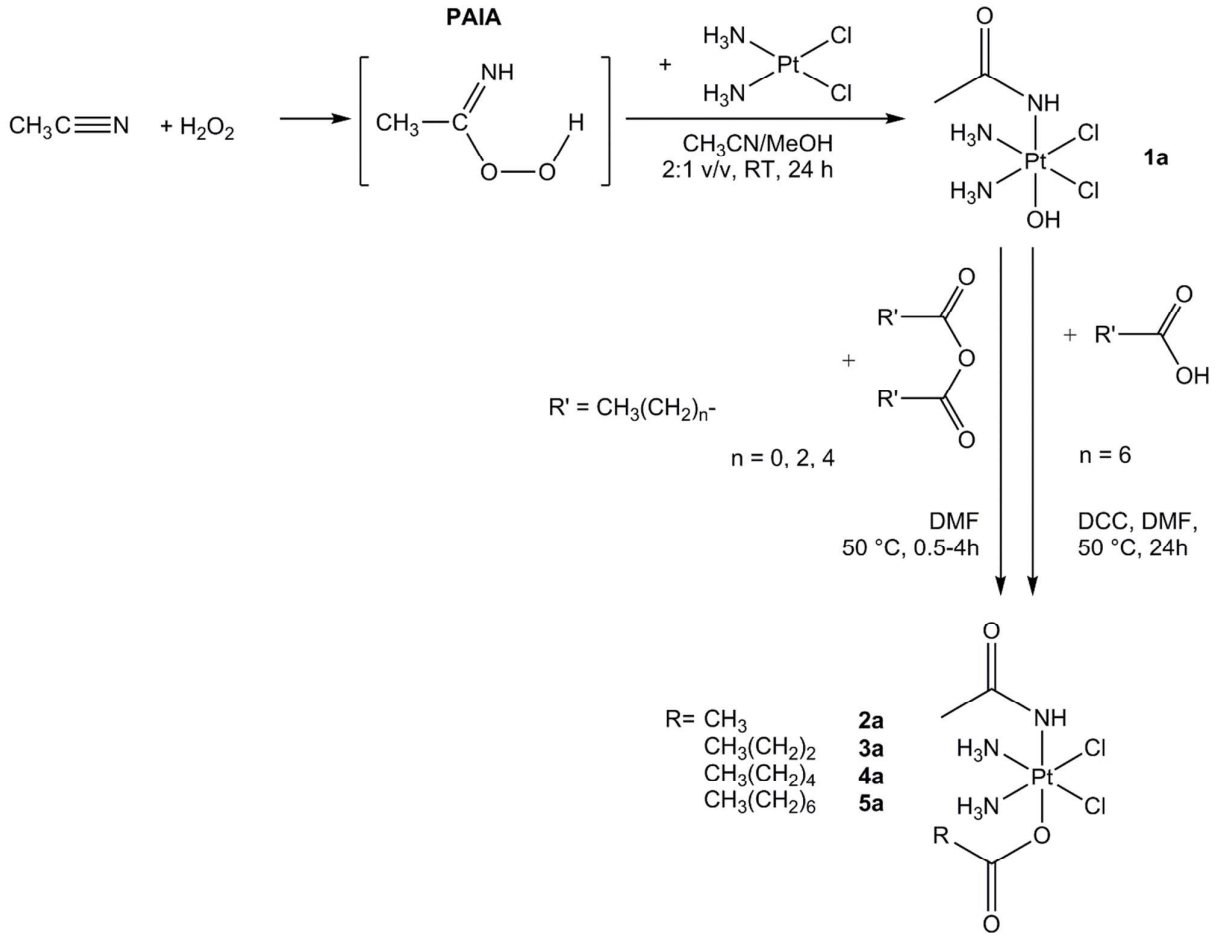

Scheme 1. Reaction scheme for the synthesis of the acetylamido complexes **1a-5a**

(DCC = dicyclohexycarbodiimide)

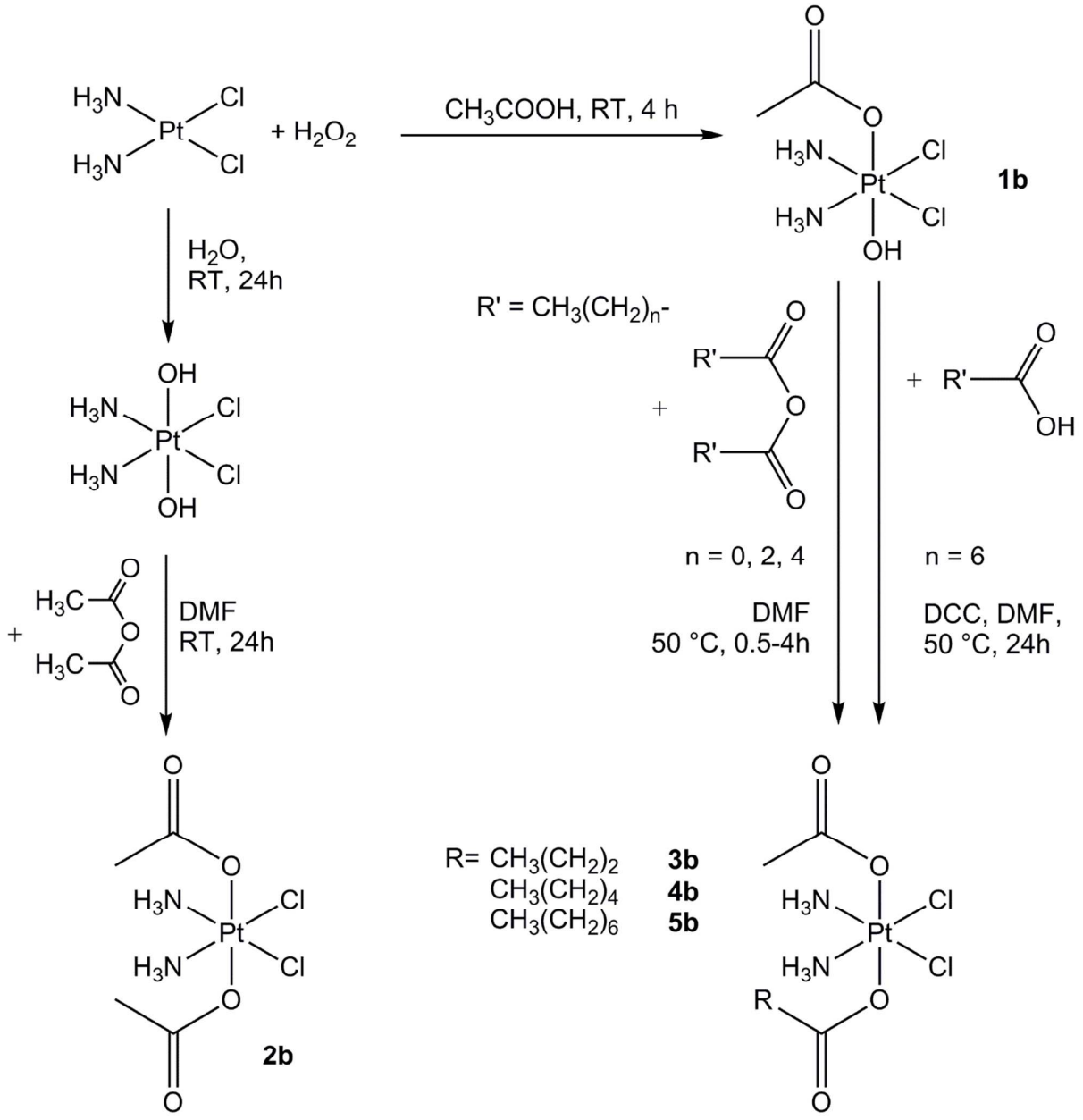

Scheme 2. Reaction scheme for the synthesis of the acetato complexes **1b-5b**

(DCC = dicyclohexycarbodiimide)

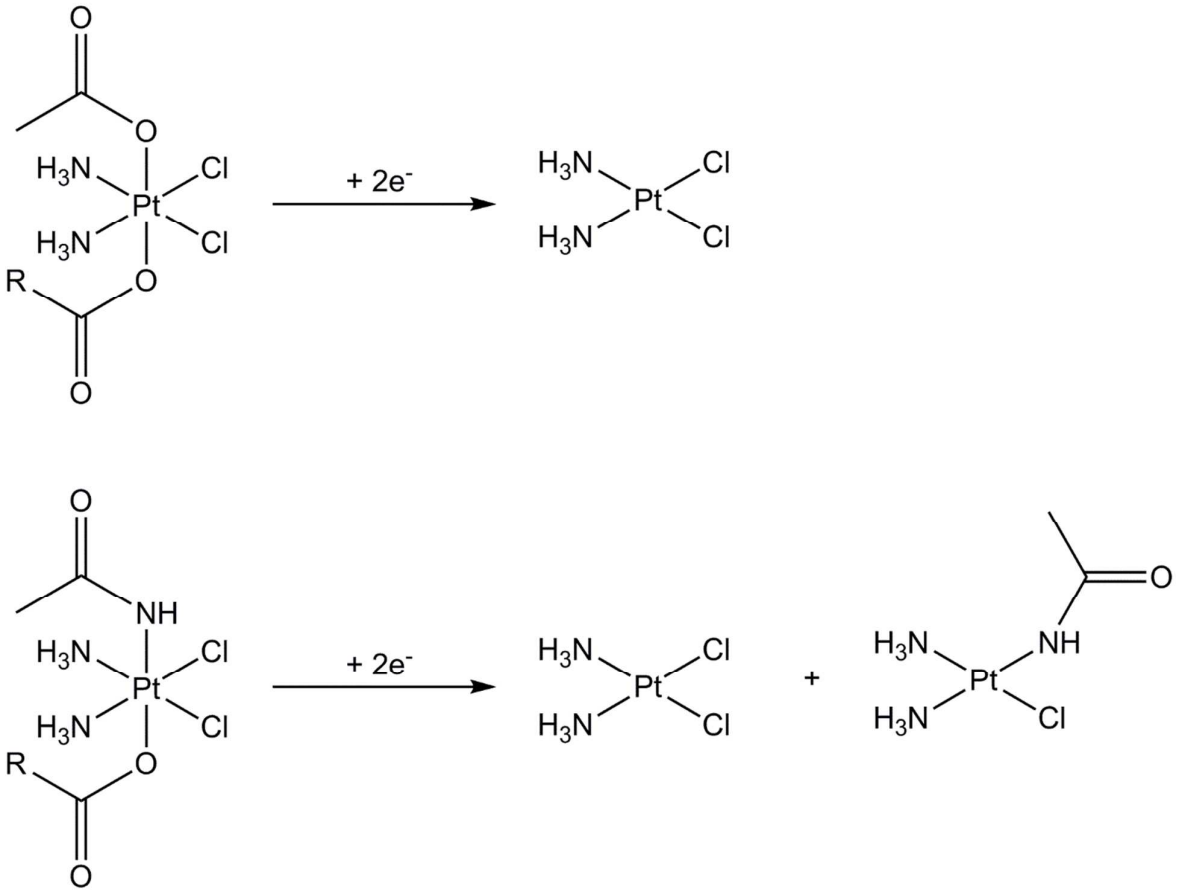

Scheme 3. General reduction scheme of complexes **a** and **b**. Hydrolyzed products and organic residues were omitted for clarity.

Antiproliferative activity of a series of cisplatin-based Pt(IV)-acetylamido/carboxylato prodrugs

Mauro Ravera,[a] Elisabetta Gabano,[a] Ilaria Zanellato,[a] Federico Fregonese,[a] Giorgio Pelosi,[b] James A. Platts,[c] Domenico Osella[a]*.

[a] *Dipartimento di Scienze e Innovazione Tecnologica*, *Università del Piemonte Orientale*, *Viale Teresa Michel 11*, *15121 Alessandria (Italy).*

[b] *Dipartimento di Chimica*, *Università di Parma*, *Parco Area delle Scienze*, *17/A*, *43124 Parma (Italy).*

[c] *School of Chemistry, Cardiff University, Park Place, Cardiff CF10 3AT (United Kingdom)*

ELECTRONIC SUPPLEMENTARY INFORMATION

Content:

* Corresponding author; e-mail address: domenico.osella@uniupo.it.

Table S1. Crystallographic data for complex **3a**.

Chemical formula	$C_6H_{17}Cl_2N_3O_3Pt$
M_r	445.21
Crystal system	Monoclinic
Space group	$P2_1/c$
Temperature / K	293
Wavelength / Å	0.71073
a / Å	10.400(2)
b / Å	10.093(2)
c / Å	13.361(2)
α / °	90.00
β / °	100.644(3)
γ / °	90.00
V / Å^3	1378.4(4)
Z	4
Density / Mg m^{-3}	2.145
Absorption co-efficient / mm^{-1}	1.056
Absorption correction	Multi-scan
F(000)	840
Total no. of reflections	3752
Reflections, $I > 2\sigma(I)$	3024
Max. 2θ / °	29.31
Ranges (h, k, l)	$-14 \le h \le 13, -13 \le k \le 13, -18 \le l \le 18$
Refinement method	Full-matrix least-squares on F^2
Goodness-of-fit on F^2	1.042
R index [$I > 2\sigma(I)$]	0.0415
R index (all data)	0.0543

Table S2. Selected bond distances (Å), angles (°) and hydrogen bonds for complex **3a**.

Pt1-N3	1.987(6)	Pt1-N2	2.036(5)
Pt1-O2	2.039(5)	Pt1-N1	2.052(7)
Pt1-Cl2	2.314(2)	Pt1-Cl1	2.325(2)
N3-C1	1.323(8)	O1-C1	1.227(9)
O2-C3	1.293(10)	C3-O3	1.206(10)
C3-C4	1.500(11)	C2-C1	1.518(10)
C4-C5	1.506(11)	C5-C6	1.548(14)
N3-Pt1-N2	92.9(2)	N3-Pt1-O2	175.6(2)
N2-Pt1-O2	91.2(2)	N3-Pt1-N1	89.8(3)
N2-Pt1-N1	89.4(2)	O2-Pt1-N1	92.0(3)
N3-Pt1-Cl2	89.8(2)	N2-Pt1-Cl2	89.22(17)
O2-Pt1-Cl2	88.53(17)	N1-Pt1-Cl2	178.58(16)
N3-Pt1-Cl1	86.89(18)	N2-Pt1-Cl1	179.65(16)
O2-Pt1-Cl1	89.05(16)	N1-Pt1-Cl1	90.30(17)
Cl2-Pt1-Cl1	91.04(7)	C1-N3-Pt1	127.6(5)
C3-O2-Pt1	123.5(5)	O3-C3-O2	125.1(8)
O3-C3-C4	121.7(9)	O2-C3-C4	113.2(9)
O1-C1-N3	123.7(7)	O1-C1-C2	120.5(7)
N3-C1-C2	115.8(7)	C3-C4-C5	116.8(10)
C4-C5-C6	109.3(14)		

Donor...Acceptor		Donor-H...Acceptor	
N1...O3 (0)	2.856(.013)	N1-H1A...O3 (0)	100.52(0.54)
N2...O3 (0)	2.885(.009)	N2-H2A...O3 (0)	131.35(0.43)
N2...O1 (0)	2.783(.009)	N2-H2C...O1 (0)	134.69(0.40)
N2...O2 (1)	3.008(.007)	N2-H2B...O2 (1)	143.27(0.37)
N1...O1 (2)	2.842(.008)	N1-H1B...O1 (2)	162.95(0.38)
N2...O1 (2)	2.963(.007)	N2-H2C...O1 (2)	131.10(0.38)

Equivalent positions: (0) x, y, z

(1) -x+1, +y+1/2, -z+1/2

(2) -x+1, -y+1, -z+1

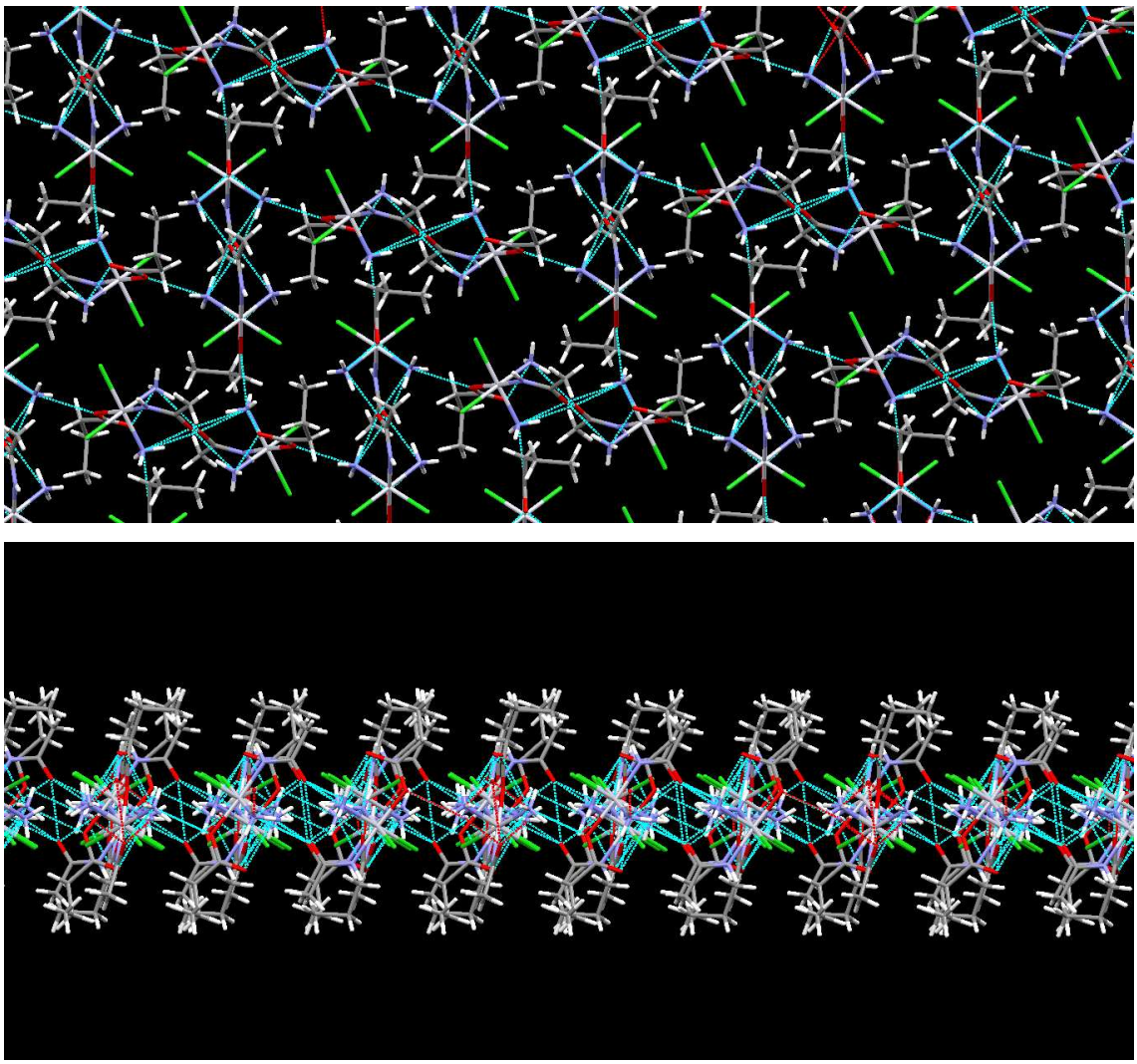

Figure S1. View of the packing looking down the *c* axis of the unit cell (above) and lateral view of the same image in which the hydrophobic tails protruding from both sides of the sheet are apparent (below).

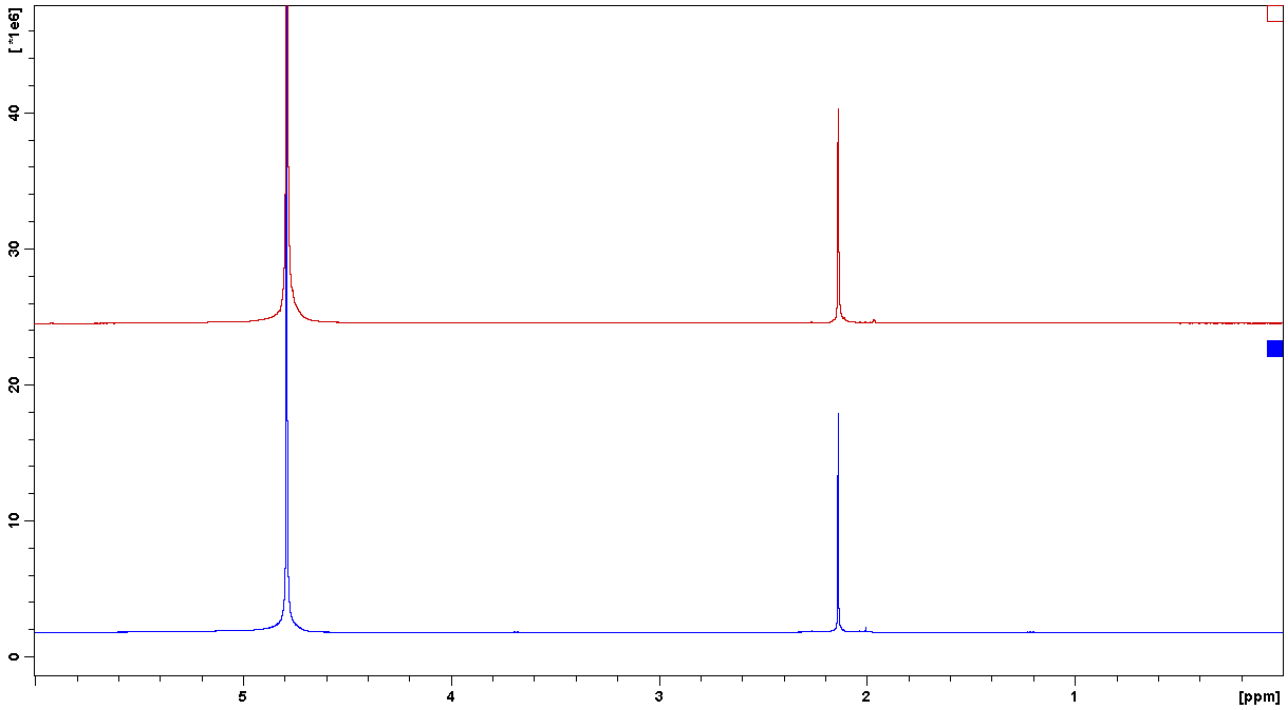

Figure S2. ^{1}H NMR spectra of **1a** (upper spectrum: fresh solution; lower spectrum: after 3 d). Solvent: phosphate buffer (PB) 100 mM in D_2O. The same results were obtained either when the samples were maintained in the dark or exposed to natural daylight cycles.

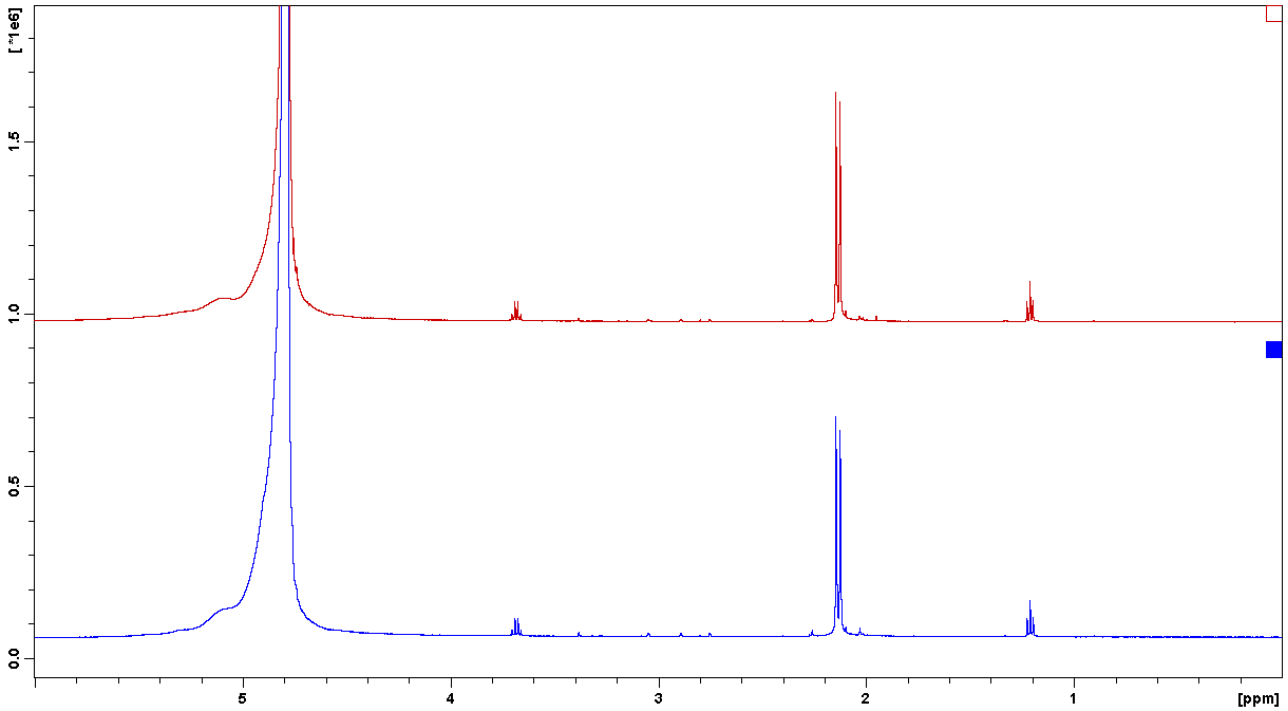

Figure S3. ^{1}H NMR spectra of **2a** (upper spectrum: fresh solution; lower spectrum: after 3 d). Solvent: PB 100 mM in D_2O. The same results were obtained either when the samples were maintained in the dark or exposed to natural daylight cycles. The signals of diethyl ether (at about 1.2 and 3.7 ppm) are also present.

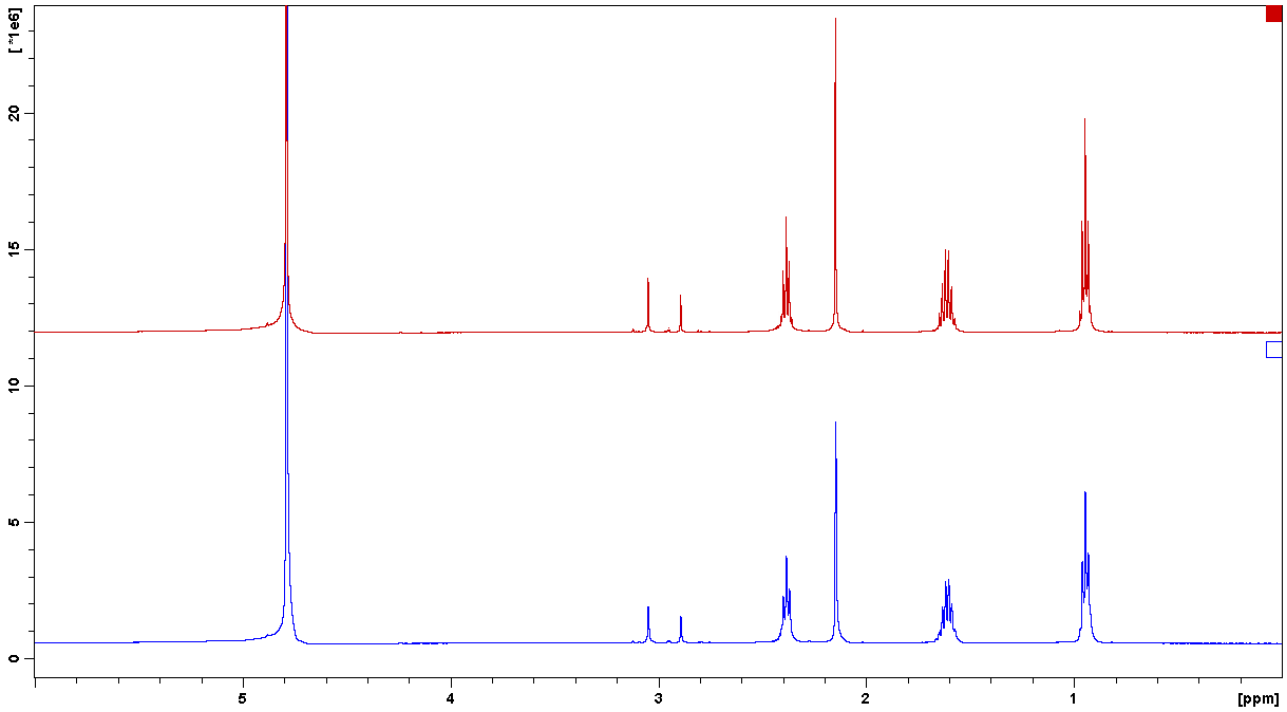

Figure S4. ^{1}H NMR spectra of **3a** (upper spectrum: fresh solution; lower spectrum: after 3 d). Solvent: PB 100 mM in D_2O. The same results were obtained either when the samples were maintained in the dark or exposed to natural daylight cycles. The signals of DMF (at about 3 ppm) are also present.

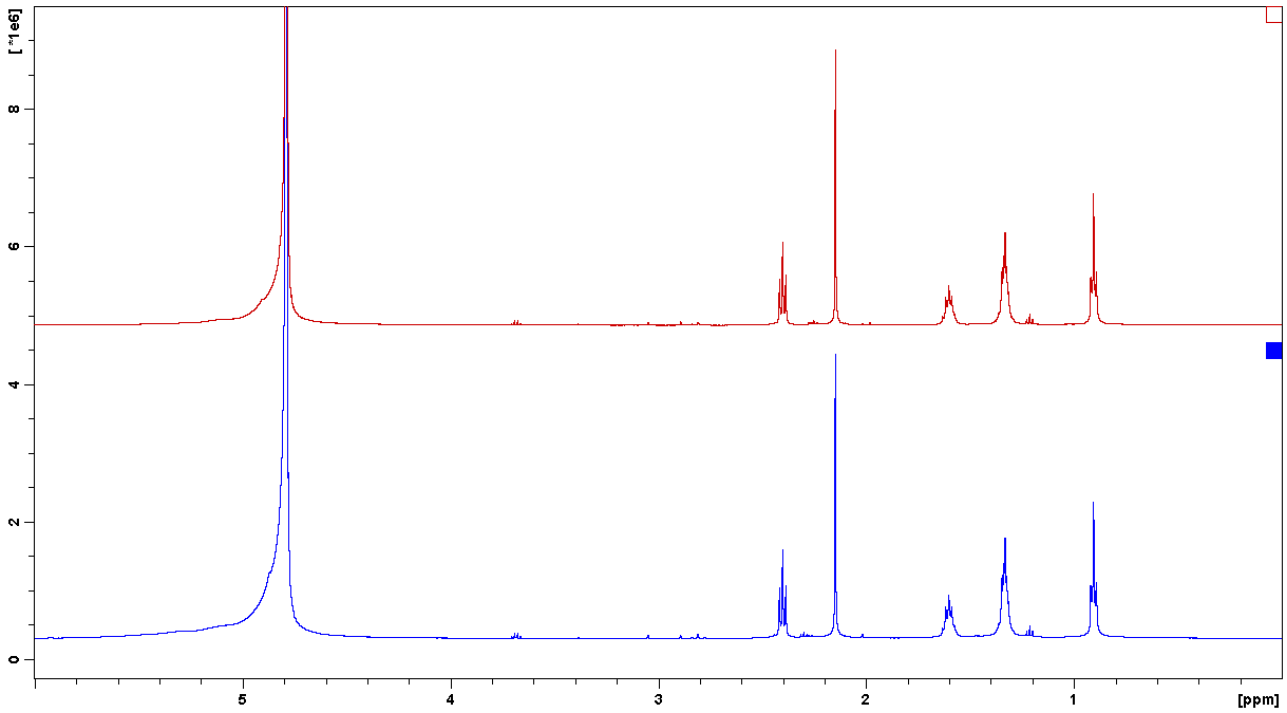

Figure S5. ^{1}H NMR spectra of **4a** (upper spectrum: fresh solution; lower spectrum: after 3 d). Solvent: PB 100 mM in D_2O. The same results were obtained either when the samples were maintained in the dark or exposed to natural daylight cycles. The signals of diethyl ether (at about 1.2 and 3.7 ppm) are also present.

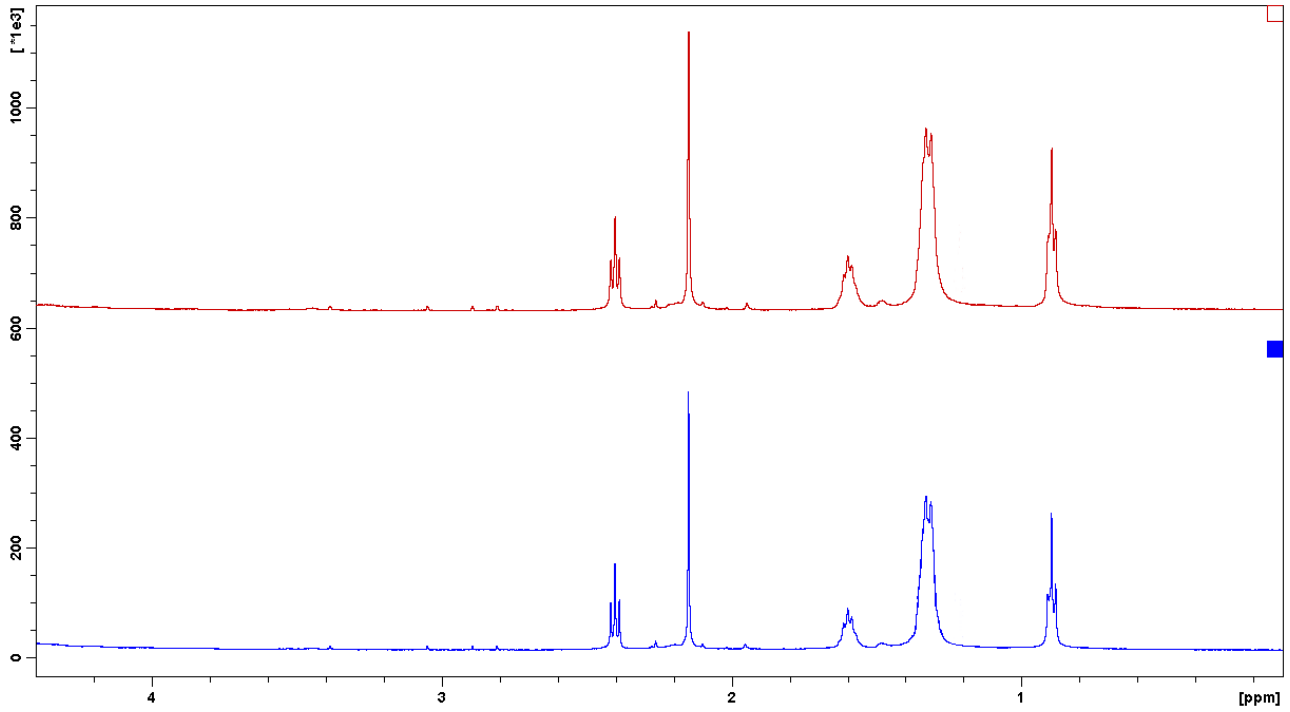

Figure S6. ^{1}H NMR spectra of **5a** (upper spectrum: fresh solution; lower spectrum: after 3 d). Solvent: PB 100 mM in D_2O. The same results were obtained either when the samples were maintained in the dark or exposed to natural daylight cycles. The signals of diethyl ether (at about 1.2 and 3.7 ppm) are also present.

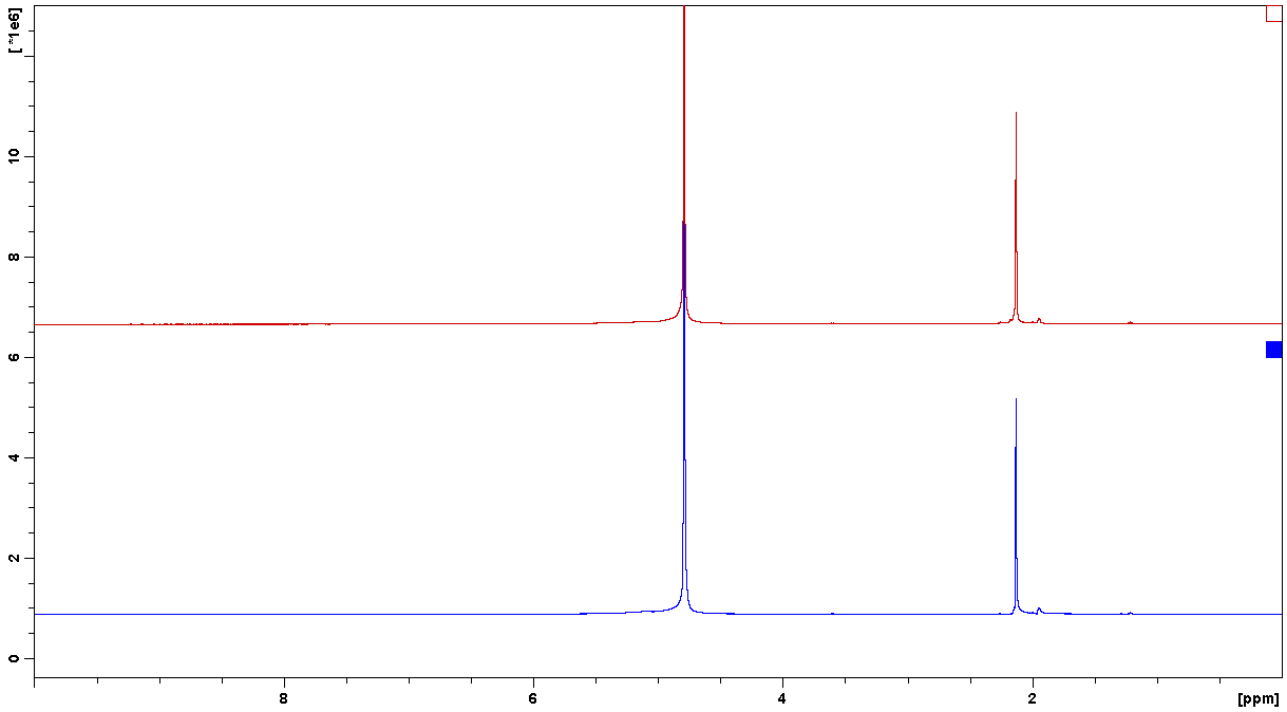

Figure S7. ^{1}H NMR spectra of **1b** maintained in the dark (upper spectrum: fresh solution; lower spectrum: after 3 d).). Solvent: PB 100 mM in D_2O.

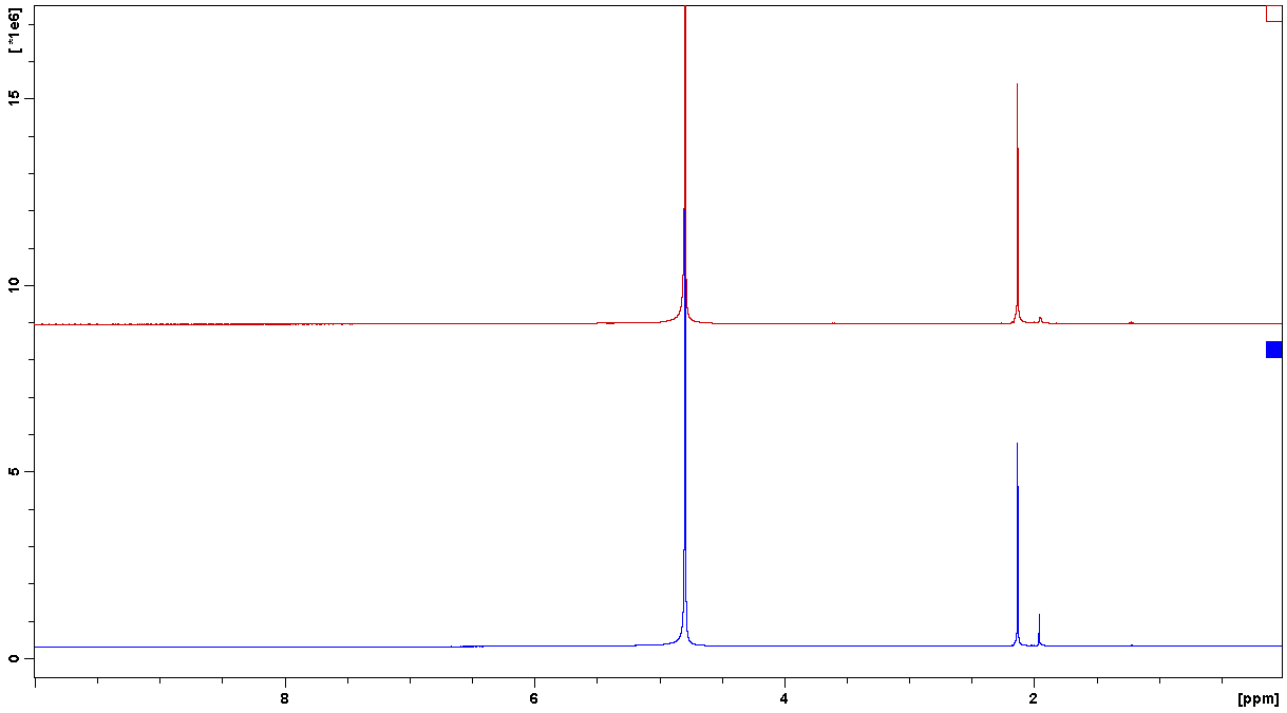

Figure S8. ^{1}H NMR spectra of **1b** exposed to natural daylight cycles (upper spectrum: fresh solution; lower spectrum: after 3 d). Solvent: PB 100 mM in D_2O.

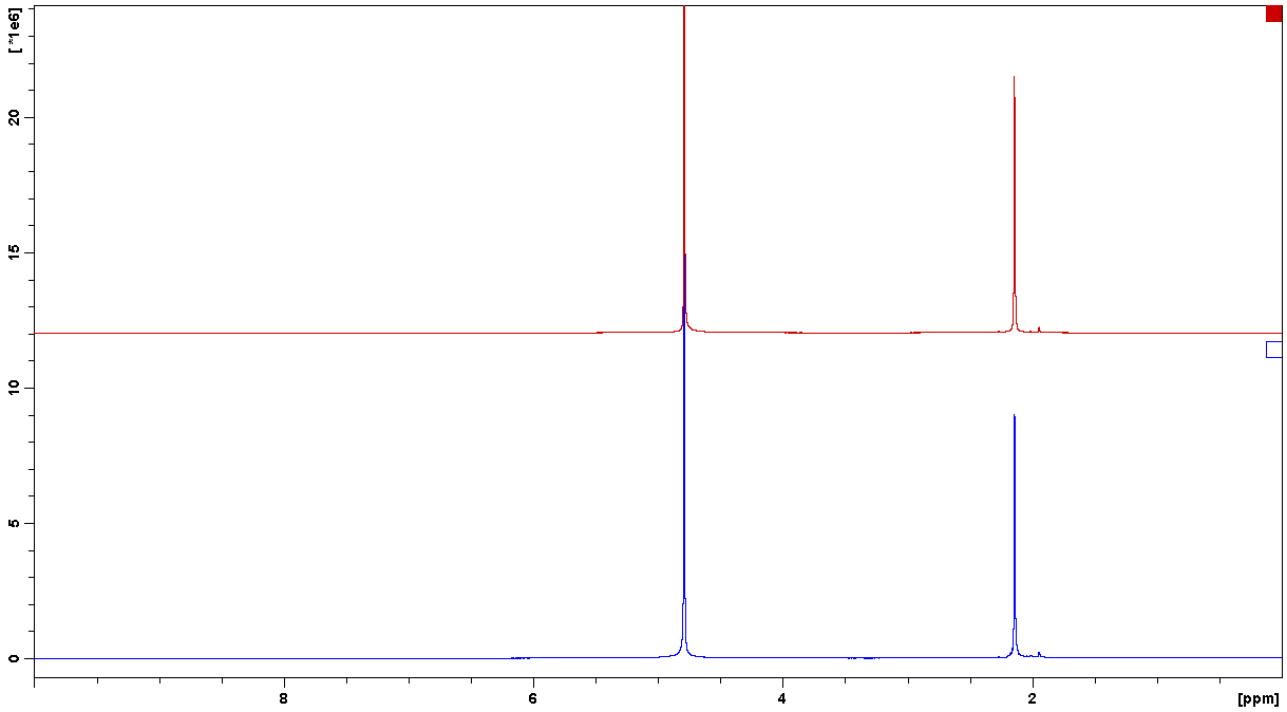

Figure S9. NMR spectra of **2b** maintained in the dark (upper spectrum: fresh solution; lower spectrum: after 3 d). Solvent: PB 100 mM in D_2O.

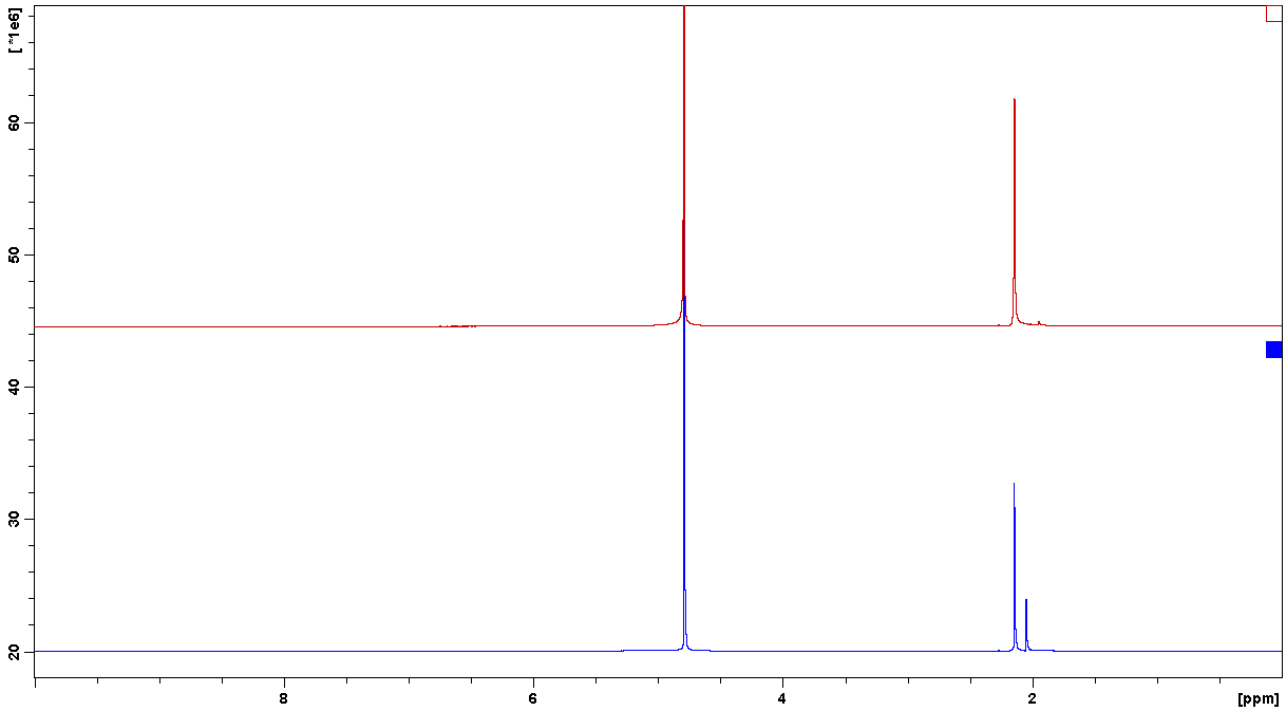

Figure S10. ^1H NMR spectra of **2b** exposed to natural daylight cycles (upper spectrum: fresh solution; lower spectrum: after 3 d). Solvent: PB 100 mM in D_2O.

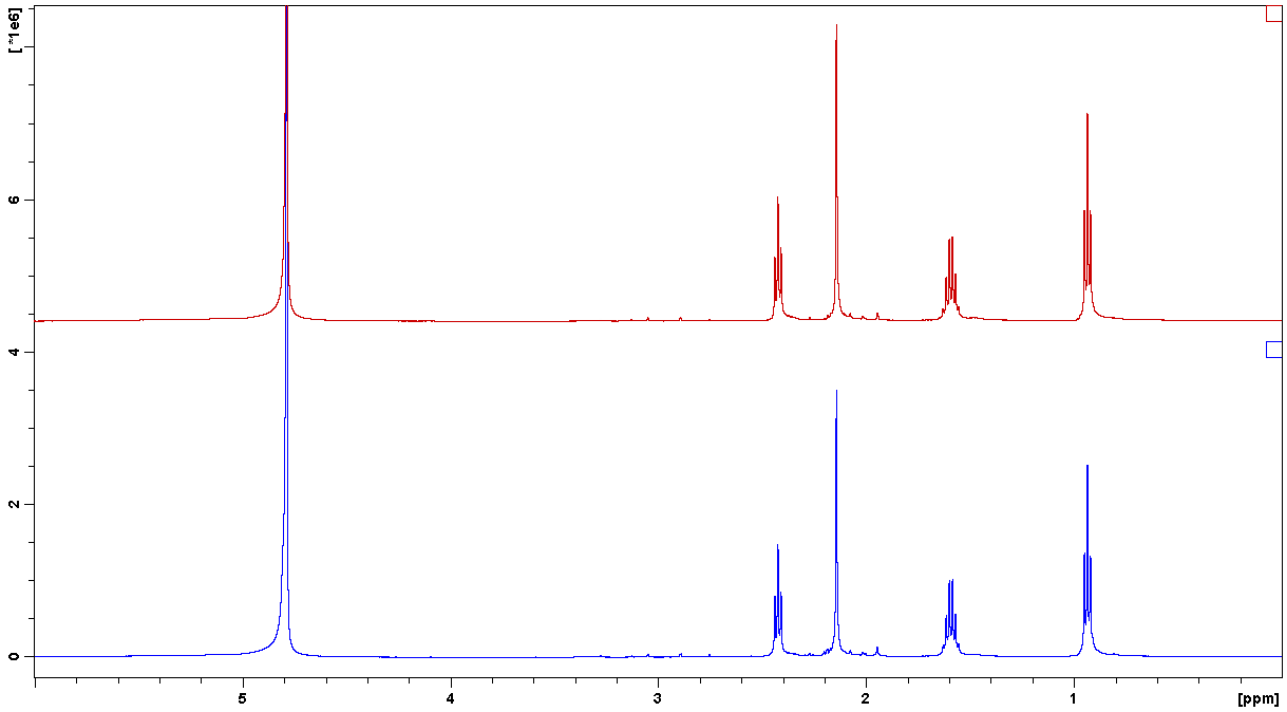

Figure S11. ^{1}H NMR spectra of **3b** (upper spectrum: fresh solution; lower spectrum: after 3 d). Solvent: PB 100 mM in D_2O. The same results were obtained either when the samples were maintained in the dark or exposed to natural daylight cycles.

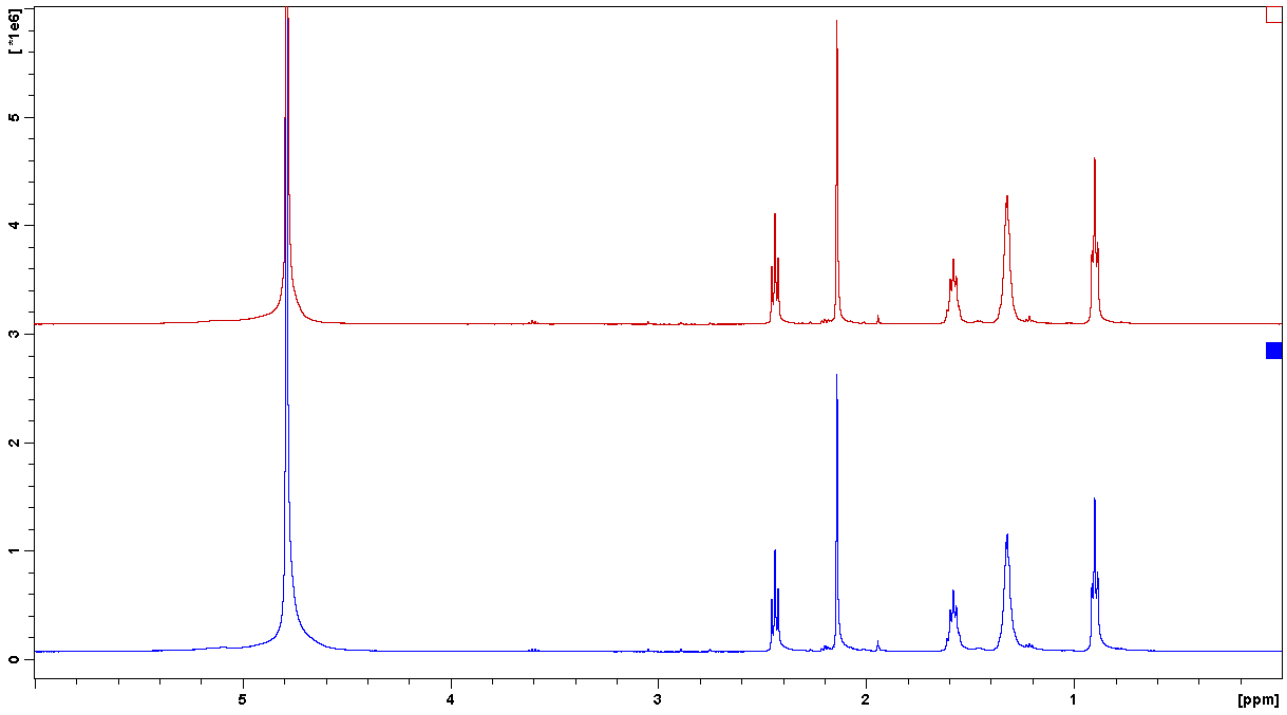

Figure S12. ^{1}H NMR spectra of **4b** (upper spectrum: fresh solution; lower spectrum: after 3 d). Solvent: PB 100 mM in D_2O. The same results were obtained either when the samples were maintained in the dark or exposed to natural daylight cycles.

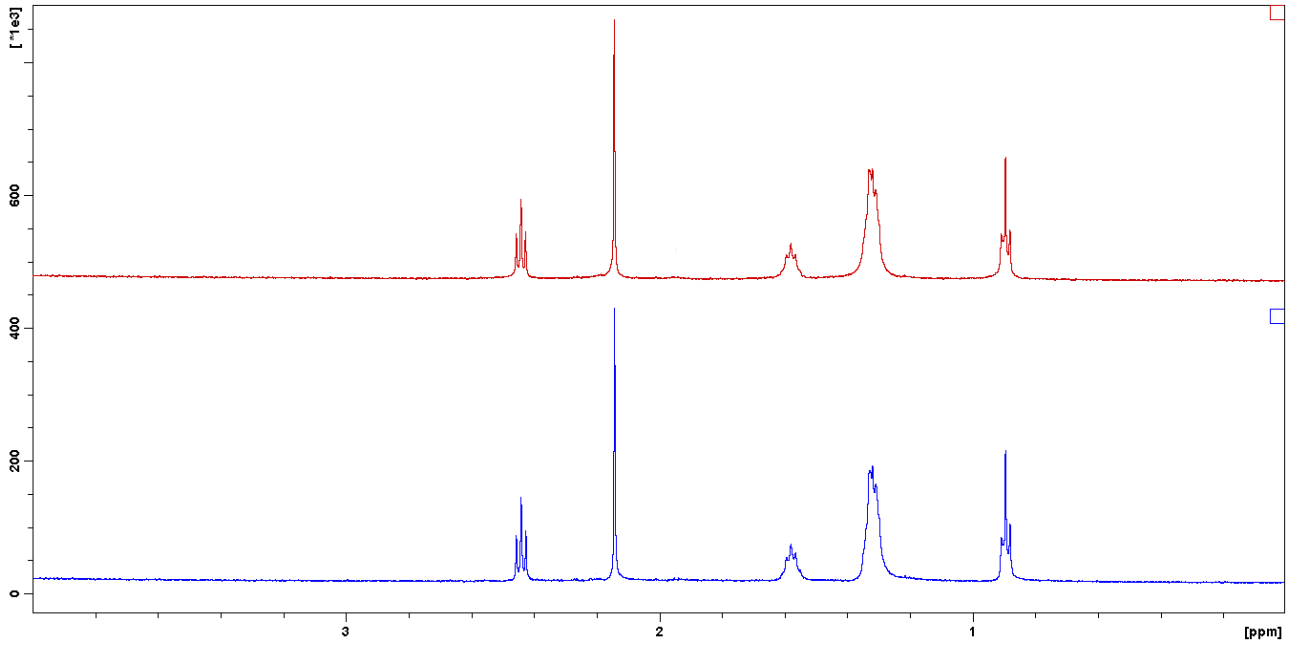

Figure S13. ^{1}H NMR spectra of **5b** (upper spectrum: fresh solution; lower spectrum: after 3 d). Solvent: PB 100 mM in D_2O. The same results were obtained either when the samples were maintained in the dark or exposed to natural daylight cycles.

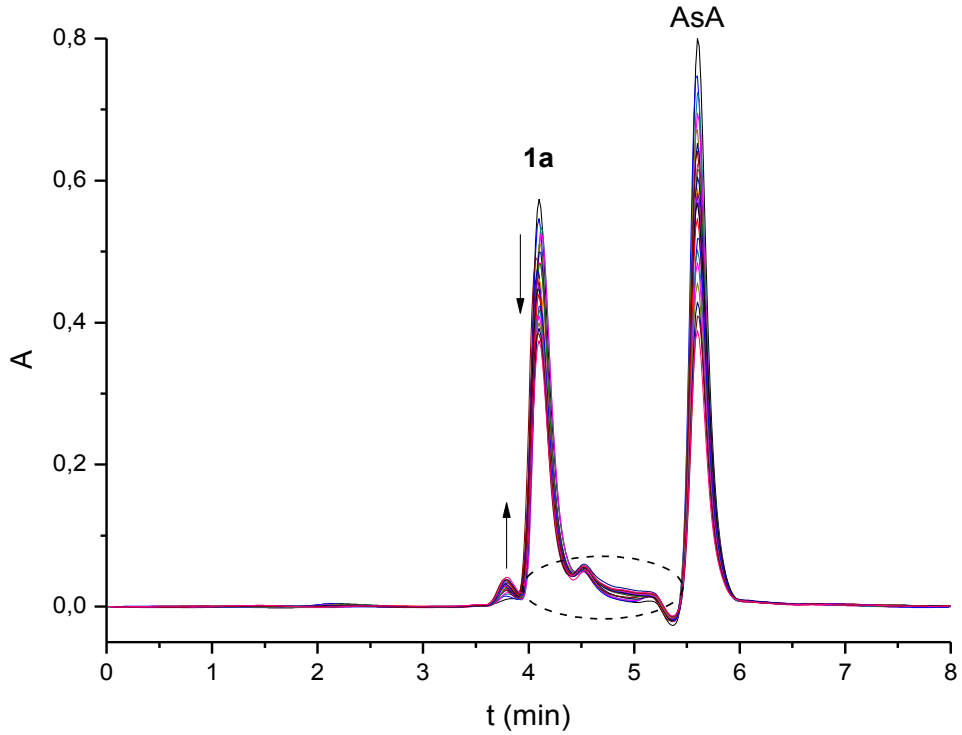

Figure S14. RP-HPLC chromatograms (eluent: 15 mM HCOOH/MeOH 70:30) of the reduction of **1a** with ascorbic acid (AsA) ([Pt] = 0.5 mM, [AsA] = 5 mM) in HEPES buffer (2 mM, pH 7.5). The peak of **1a** (4.1 min) decreases over the time, whereas a new peak at 3.8 min increases (its ESI-MS corresponds to $[Pt(acetamidato\text{-}N)(NH_3)_2]^+$ together with fragmentations of hydrolyzed cisplatin). In the region inside the circle, some different peaks overlap (HEPES buffer, cisplatin and $[Pt(acetamidato\text{-}N)Cl(NH_3)_2]$). The presence of this last species is confirmed by the chromatograms of the other **a** complexes, as in the case of **3a** (see Fig. S16), where this peak (4.06 min) is not overlapped to that of the original Pt(IV) complex. The ESI-MS spectrum of $[Pt(acetamidato\text{-}N)Cl(NH_3)_2]$ is reported in Fig. S24.

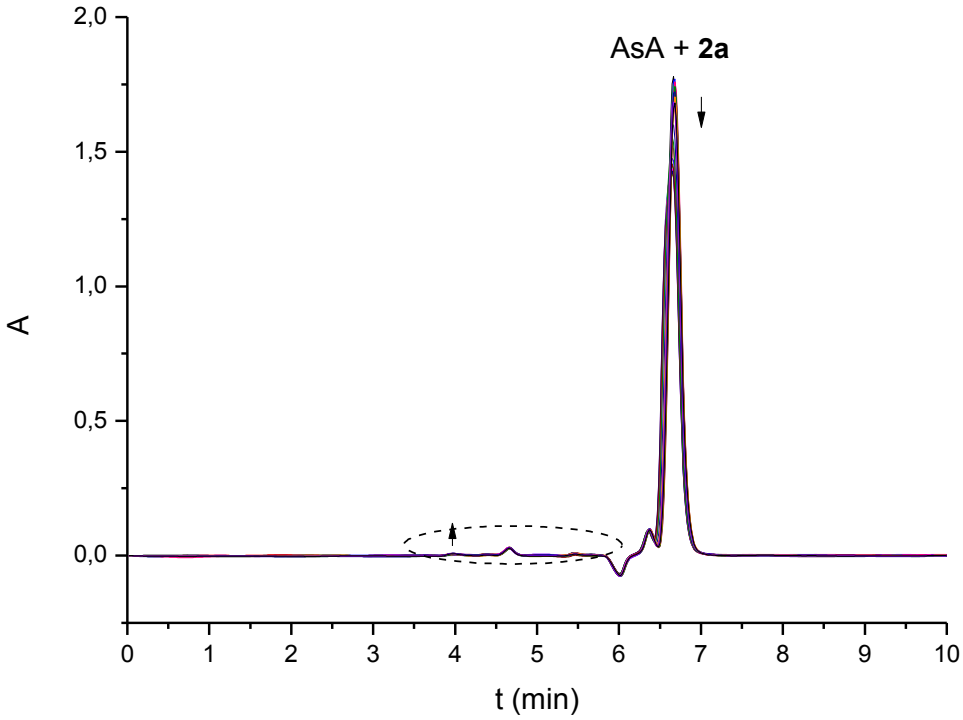

Figure S15. RP-HPLC chromatograms (eluent: 15 mM HCOOH/MeOH 90:10) of the reduction of **2a** with AsA ([Pt] = 0.5 mM, [AsA] = 5 mM) in HEPES buffer (2 mM, pH 7.5). The peak of **2a** slightly decreases but overlaps that of AsA. In the region inside the circle, some different peaks overlap (HEPES buffer, cisplatin and its hydrolyzed derivatives).

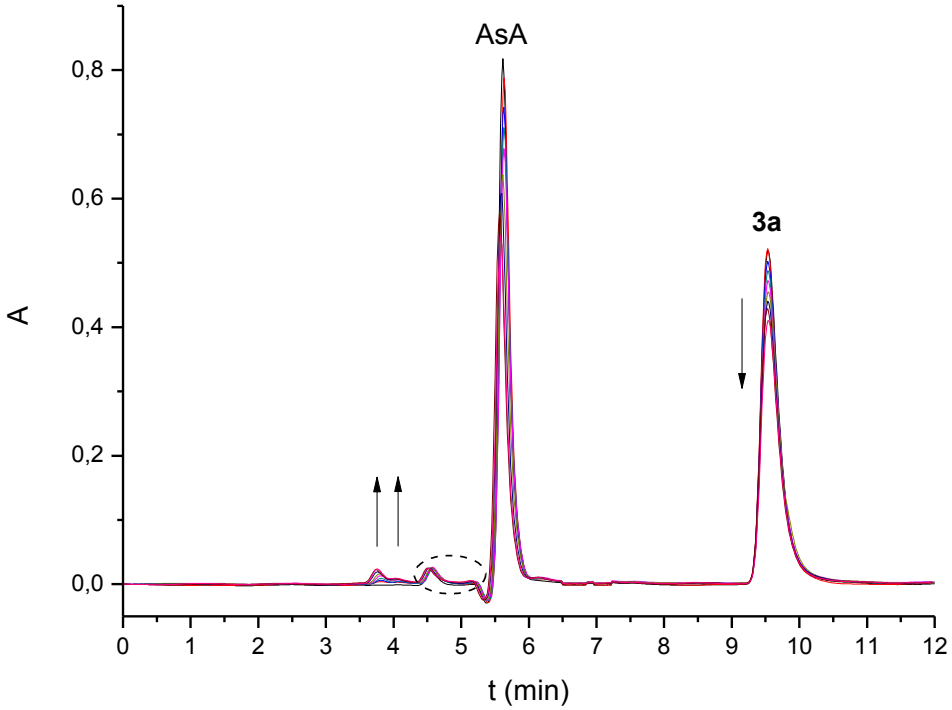

Figure S16. RP-HPLC chromatograms (eluent: 15 mM HCOOH/MeOH 70:30) of the reduction of **3a** with AsA ([Pt] = 0.5 mM, [AsA] = 5 mM) in HEPES buffer (2 mM, pH 7.5). The peak at 4.06 min, not overlapped to that of the original Pt(IV) complex (9.53 min), is compatible with [Pt(acetamidato-*N*)Cl(NH_3)$_2$], as indicated by the corresponding ESI-MS spectrum (Fig. S24). In the region inside the circle, HEPES buffer and cisplatin overlap.

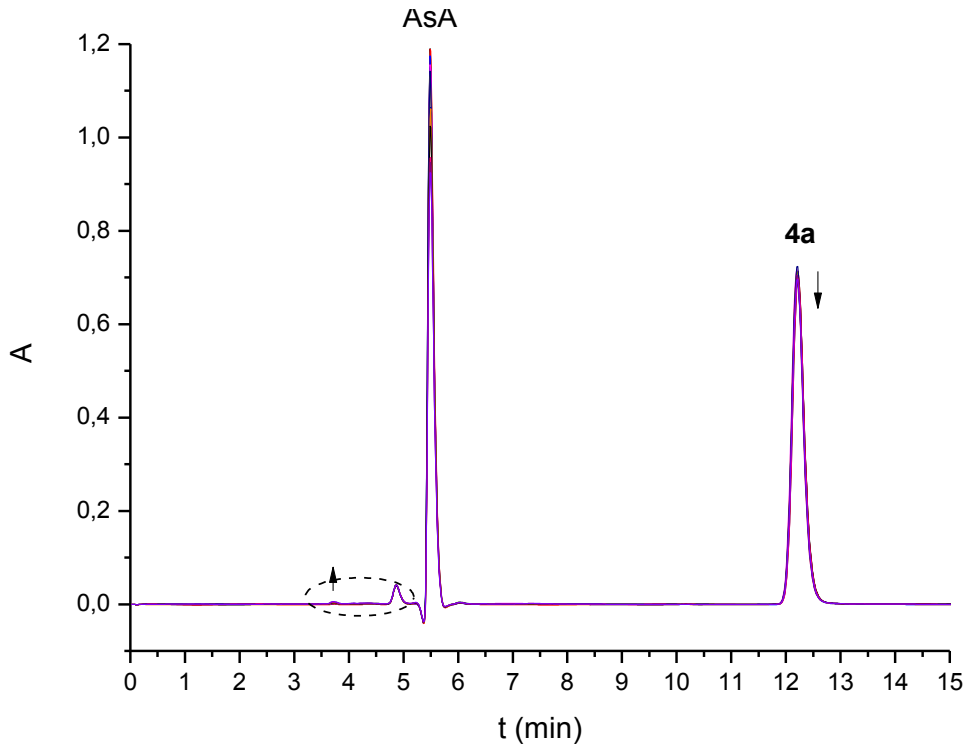

Figure S17. RP-HPLC chromatograms (eluent: 15 mM HCOOH/MeOH 50:50) of the reduction of **4a** with AsA ([Pt] = 0.5 mM, [AsA] = 5 mM) in HEPES buffer (2 mM, pH 7.5). The peak of **4a** slightly decreases over the time. In the region inside the circle, some different peaks overlap (HEPES buffer, cisplatin and its hydrolyzed derivatives).

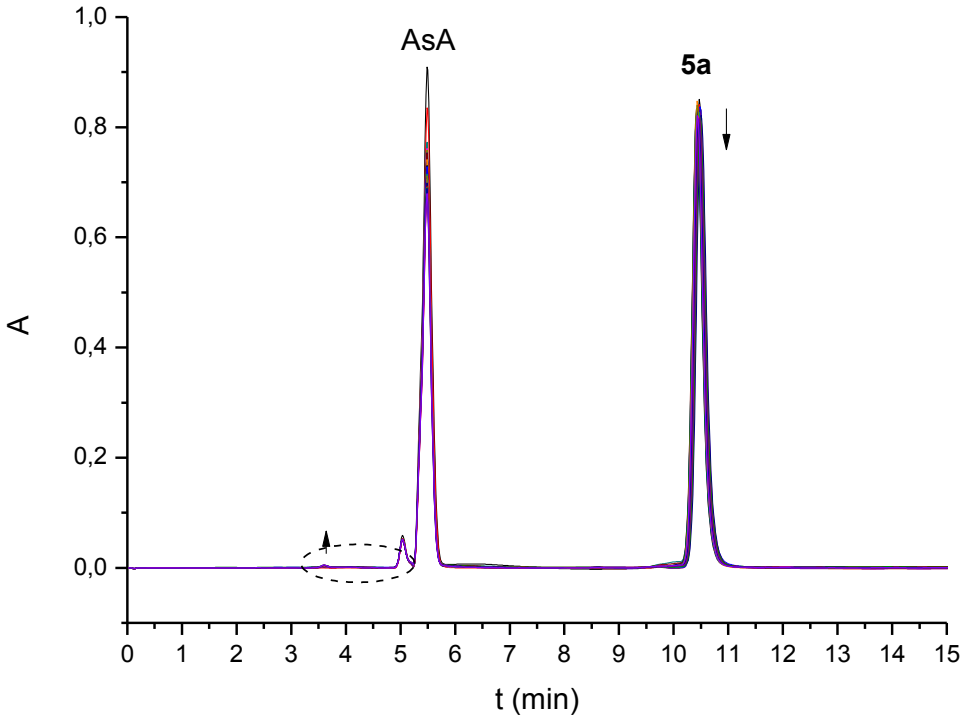

Figure S18. RP-HPLC chromatograms (eluent: 15 mM HCOOH/MeOH 30:70) of the reduction of **5a** with AsA ([Pt] = 0.5 mM, [AsA] = 5 mM) in HEPES buffer (2 mM, pH 7.5). The peak of **5a** slightly decreases over the time. In the region inside the circle, some different peaks overlap (HEPES buffer, cisplatin and its hydrolyzed derivatives).

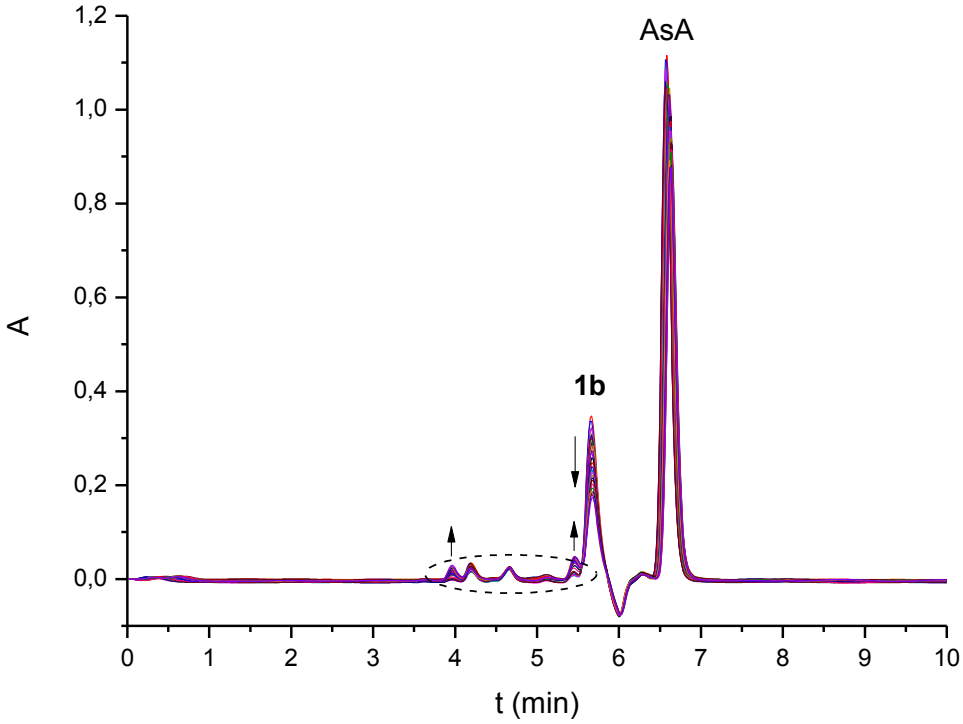

Figure S19. RP-HPLC chromatograms (eluent: 15 mM HCOOH/MeOH 90:10) of the reduction of **1b** with AsA ([Pt] = 0.5 mM, [AsA] = 5 mM) in HEPES buffer (2 mM, pH 7.5). The peak of **1b** decreases over the time, whereas new peaks increases in the region inside the circle, where some different peaks overlap (HEPES buffer, cisplatin and its hydrolyzed species).

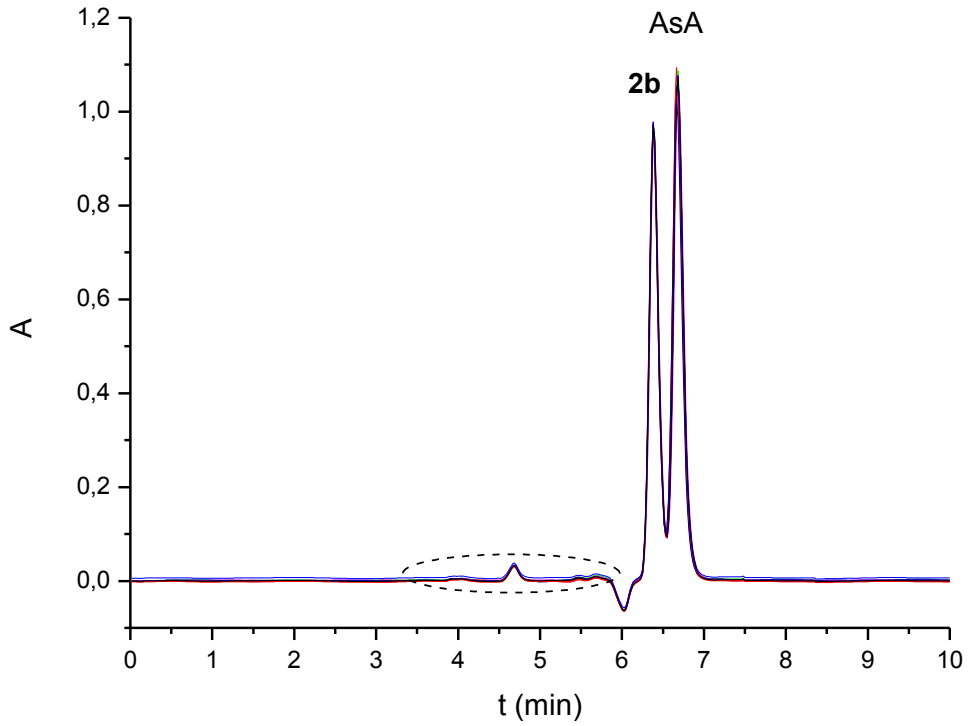

Figure S20. RP-HPLC chromatograms (eluent: 15 mM HCOOH/MeOH 90:10) of the reduction of **2b** with AsA ([Pt] = 0.5 mM, [AsA] = 5 mM) in HEPES buffer (2 mM, pH 7.5). The peak of **2b** undergoes a very little decrease over the time. In the region inside the circle, some different peaks overlap (HEPES buffer, cisplatin and its hydrolyzed derivatives).

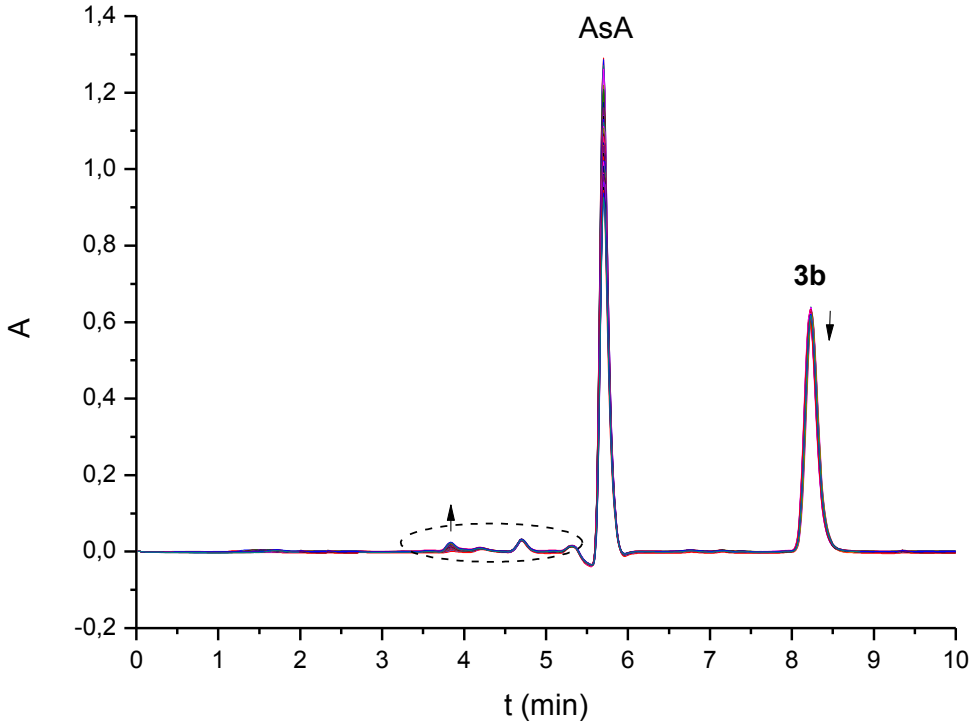

Figure S21. RP-HPLC chromatograms (eluent: 15 mM HCOOH/MeOH 70:30) of the reduction of **3b** with AsA ([Pt] = 0.5 mM, [AsA] = 5 mM) in HEPES buffer (2 mM, pH 7.5). The peak of **3b** slightly decreases over the time. In the region inside the circle, some different peaks overlap (HEPES buffer, cisplatin and its hydrolyzed derivatives).

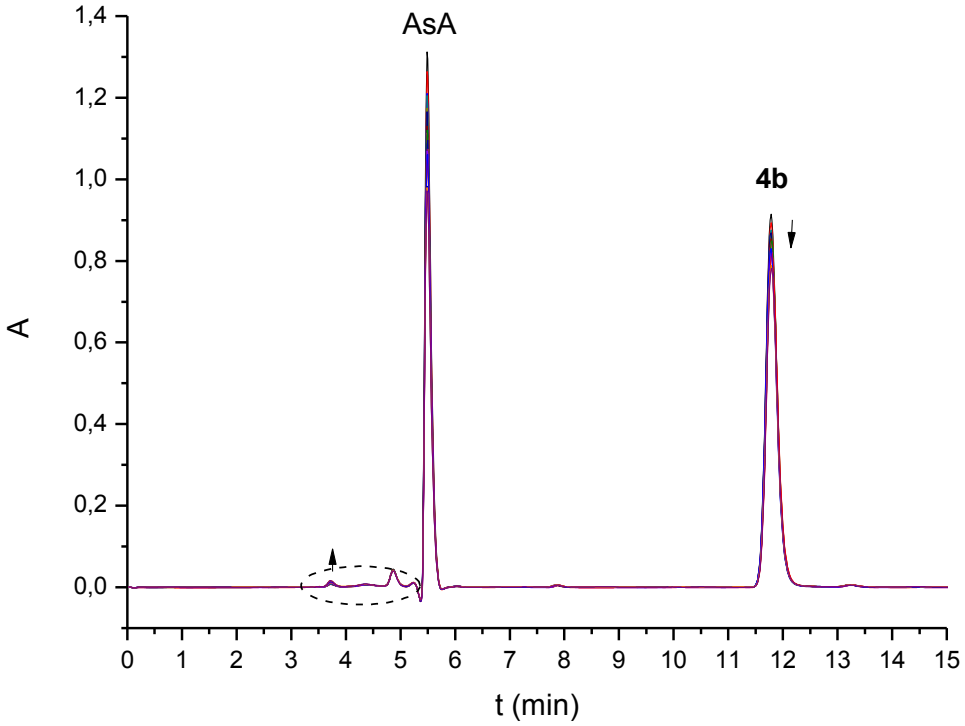

Figure S22. RP-HPLC chromatograms (eluent: 15 mM HCOOH/MeOH 50:50) of the reduction of **4b** with AsA ([Pt] = 0.5 mM, [AsA] = 5 mM) in HEPES buffer (2 mM, pH 7.5). The peak of **4b** slightly decreases over the time. In the region inside the circle, some different peaks overlap (HEPES buffer, cisplatin and its hydrolyzed derivatives).

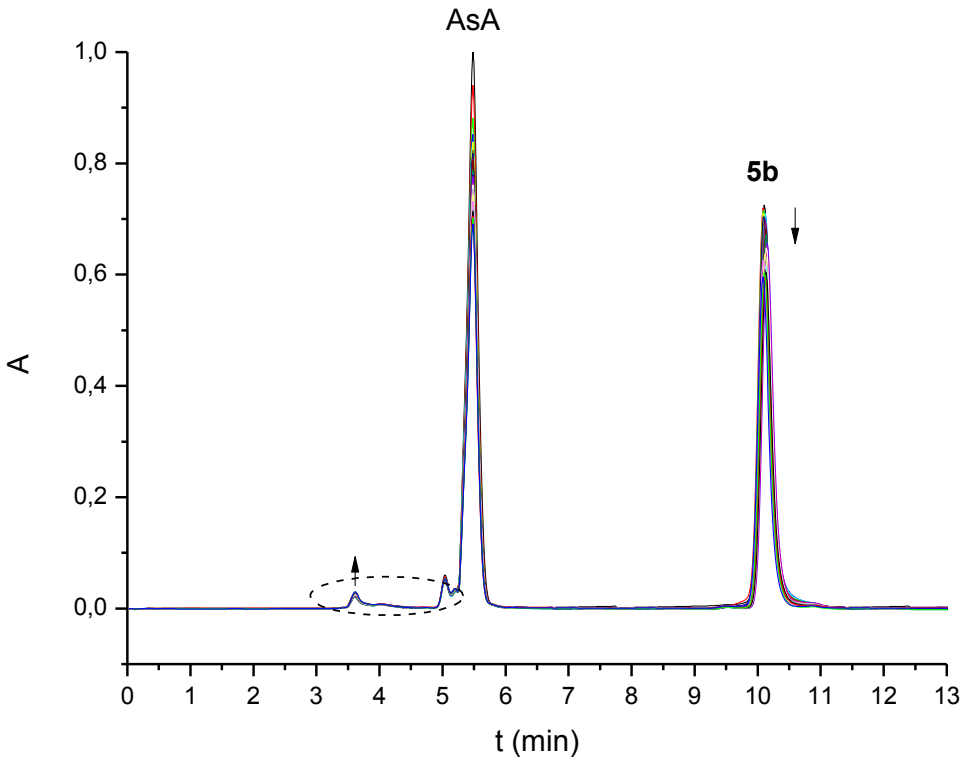

Figure S23. RP-HPLC chromatograms (eluent: 15 mM HCOOH/MeOH 30:70) of the reduction of **5b** with AsA ([Pt] = 0.5 mM, [AsA] = 5 mM) in HEPES buffer (2 mM, pH 7.5). The peak of **5b** slightly decreases over the time. In the region inside the circle, some different peaks overlap (HEPES buffer, cisplatin and its hydrolyzed derivatives).

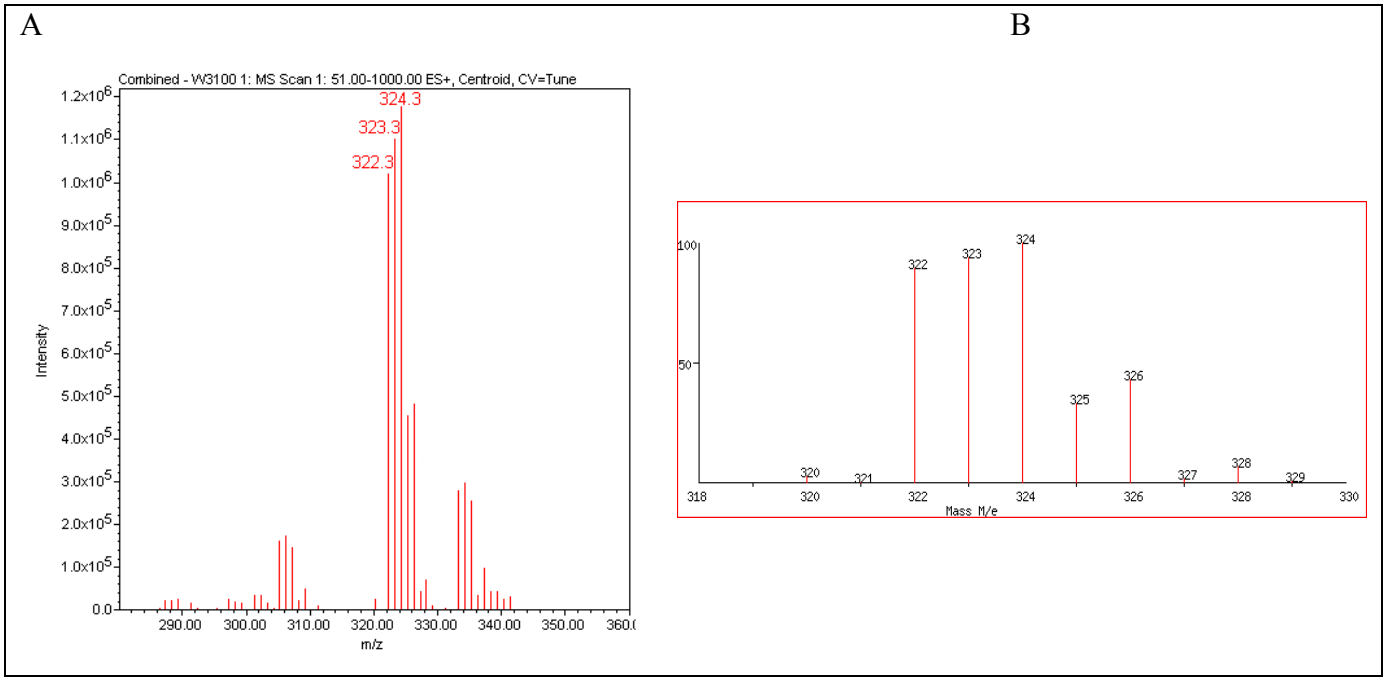

Figure S24. A) ESI-MS spectrum of [Pt(acetamidato-*N*)Cl(NH_3)$_2$] obtained as byproduct of the reduction of the **a** complexes (see Figs. S2 and S3). The spectrum shows the peak corresponding to $[M+H]^+$ at 324.3 m/z, and its fragmentations $[M-Cl+H_2O]^+$ at 306.2 m/z and $[M-Cl+HCOOH]^+$ at 334.3 m/z. B) MS simulation for $C_2H_{11}ClN_3OPt$ as $[M+H]^+$.

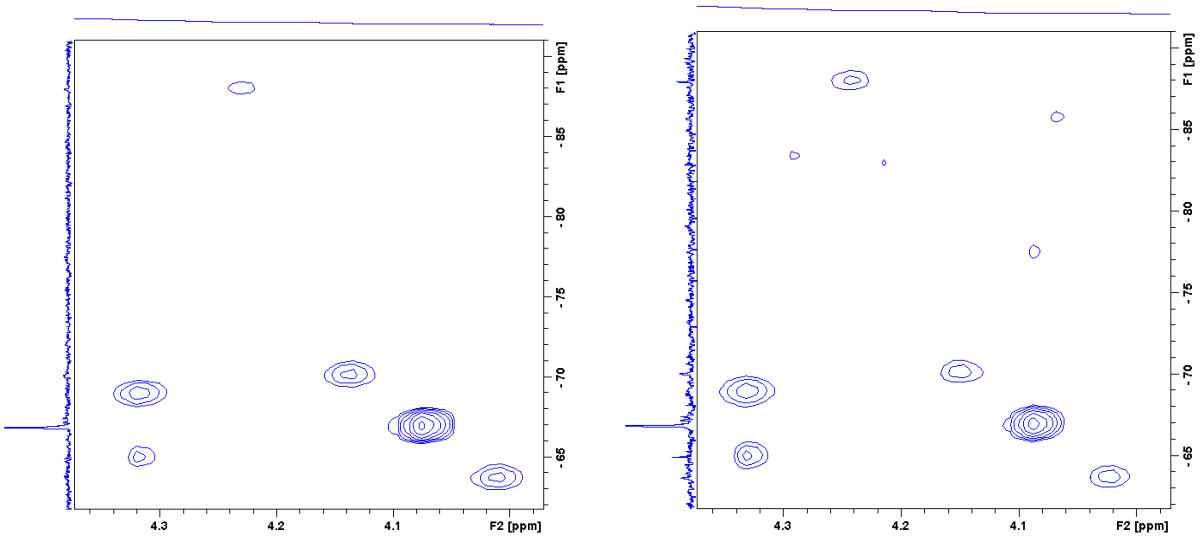

Figure S25. [^{1}H, ^{15}N] HSQC spectrum of the reduction of **1a** (20 mM) in the presence of AsA (40 mM) in 80 mM HEPES with 10% v/v D_2O and 5 mM [Cl^-] after 1 h (left) and 4 h (right) reaction time, respectively.

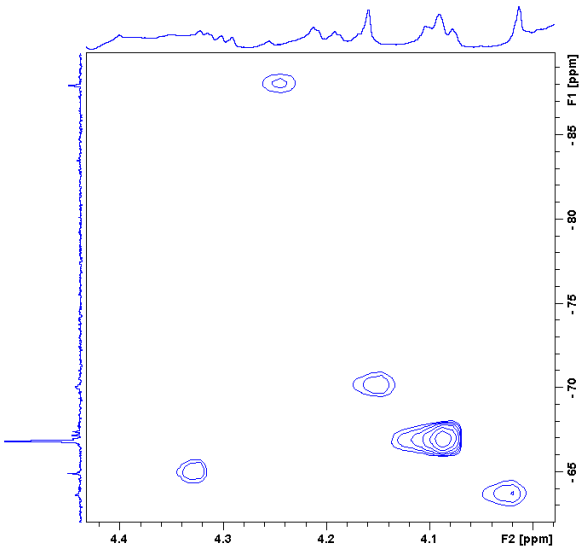

Figure S26. [^{1}H, ^{15}N] HSQC spectrum of the reduction of **1b** (20 mM) in the presence of AsA (40 mM) in 80 mM HEPES with 10% v/v D_2O and 5 mM [Cl^-] after 4 h reaction time.

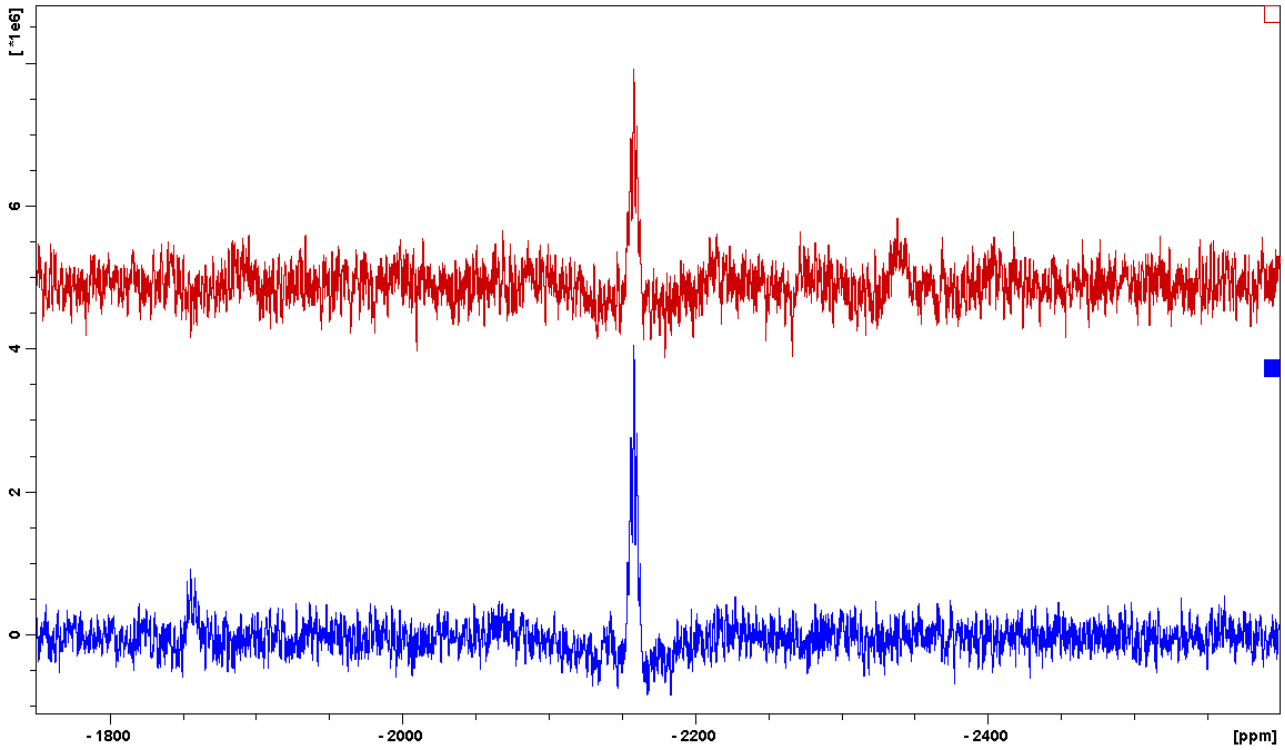

Figure S27. ^{195}Pt NMR spectra of reduction of **1a** (20 mM) in the presence of AsA (40 mM) in 80 mM HEPES with 10% v/v D_2O and 5 mM [Cl^-] after 6 h (lower spectrum) and 18 h (upper spectrum) reaction time.

Table S3. Miscellaneous experimental chemical and biological data of the complexes under investigation.

Compound	solubility [mM][a]	E_p [V][b]	t_R [min][c]	IC_{50} [μM][d]	AR[d]
cisplatin	-	-	5.2	0.48±0.11	1.40±0.57
2a	108±9	-0.660	5.4	33.1±4.7	0.77±0.21
3a	37.9±0.1	-0.688	6.8	11.8±1.9	0.63±0.15
4a	9.6±0.1	-0.681	14.4	0.20±0.02	4.44±0.11
5a	1.8±0.1	-0.702	56.8	0.04±0.01	8.47±0.94
2b	105±10	-0.486	5.5	12.1±5.2[e]	0.26±0.13
3b	27.0±0.4	-0.512	6.7	2.85±0.36	0.77±0.13
4b	8.1±0.1	-0.547	14.1	0.31±0.15	5.08±0.81
5b	3.8±0.2	-0.526	54.4	0.11±0.05	7.80±1.69

[a] The water solubility data were determined from saturated solutions of the Pt(IV) complexes in milliQ water. After 24 h stirring in the dark at 25 °C, the solid residue was filtered off (0.20 μm regenerated cellulose filters) and the Pt content of the solutions was determined by means of ICP-OES.

[b] Reduction peak potentials (E_p) were measured at a glassy carbon working electrode in ethanol solutions containing 0.1 M $[NBu_4][ClO_4]$ as supporting electrolyte. Scan rate = 0.2 V s^{-1}. All potentials are reported in V *vs.* Ag/AgCl, 3 M KCl.

[c] HPLC retention times (t_R) were measured on a C18 column, by using a mobile phase containing 15 mM aqueous HCOOH and CH_3OH in 1:1 ratio.

[d] Half-inhibitory concentrations (IC_{50}) and accumulation ratios (AR) were measured on A2780 ovarian cancer cell lines, after 72 h and 4 h of treatment, respectively.

[e] data from I. Zanellato, I. Bonarrigo, D. Colangelo, E. Gabano, M. Ravera, M. Alessio and D. Osella, *J. Inorg. Biochem.*, 2014, **140**, 219-227.

See Experimental section for more details.